

## Lehigh University Lehigh Preserve

---

Fritz Laboratory Reports

Civil and Environmental Engineering

---

1987

# Cyclic behavior of beam-to-column weak-axis moment connections, M.S. thesis, May 1987, 81p.

Kenneth A. Heaton

Follow this and additional works at: <http://preserve.lehigh.edu/engr-civil-environmental-fritz-lab-reports>

---

### Recommended Citation

Heaton, Kenneth A., "Cyclic behavior of beam-to-column weak-axis moment connections, M.S. thesis, May 1987, 81p." (1987). *Fritz Laboratory Reports*. Paper 2306.  
<http://preserve.lehigh.edu/engr-civil-environmental-fritz-lab-reports/2306>

This Technical Report is brought to you for free and open access by the Civil and Environmental Engineering at Lehigh Preserve. It has been accepted for inclusion in Fritz Laboratory Reports by an authorized administrator of Lehigh Preserve. For more information, please contact [preserve@lehigh.edu](mailto:preserve@lehigh.edu).

504.3

**CYCLIC BEHAVIOR OF BEAM-TO-COLUMN  
WEAK-AXIS MOMENT CONNECTIONS**

by

**Kenneth A. Heaton**

**FRITZ ENGINEERING  
LABORATORY LIBRARY**

A Thesis

Presented to the Graduate Committee

of Lehigh University

in Candidacy for the Degree of

Master of Science

in

Civil Engineering

Lehigh University

Bethlehem, Pennsylvania

May 1987

CERTIFICATE OF APPROVAL

This thesis is accepted and approved in partial fulfillment of the requirements for the degree of Master of Science in Civil Engineering.

May 18, 1987  
Date

-----  
George C. Driscoll  
Professor in Charge

-----  
~~Irwin J. Kugelman~~  
~~Department Chairman~~

## Acknowledgments

The analytical and experimental study presented in this thesis was conducted at Fritz Engineering Laboratory, Lehigh University, Bethlehem, Pennsylvania. Dr. Irwin J. Kugelman is chairman of the Department of Civil Engineering.

The experiments conducted in this work form part of the investigations "Cyclic Behavior of Moment Connections" sponsored by the National Science Foundation (Grant No. ECE-8320540).

The author wishes to express his sincere thanks to Dr. George C. Driscoll, supervisor of the thesis and related research work, for the benefit of his helpful suggestions and encouragement, patience and guidance during the course of this study, and demonstrating to the author both the objectivity of science and the science of humor.

Many thanks are due to Dr. Le-Wu Lu, Dr. Lynn S. Beedle, and Dr. Bruce R. Somers for their valuable ideas and suggestions during the different phases of the research project. Many people helped in the preparation of specimens, erection of the assemblage, and in the actual testing, especially Dr. Roger G. Slutter, and Messrs. Hugh T. Sutherland, Robert R. Dales, Charles F. Hittinger, Raymond Kromer, Russell Longenbach, Daniel Pense, Dave Kurtz, Gene Matlock and Todd Anthony. Mr. Richard N. Sopko took all test photographs and prepared the prints and slides. The assistance of Ms. Eleanor Nothelfer in obtaining various articles will never be forgotten.

# Table of Contents

<b>Acknowledgments</b>	<b>ii</b>
<b>Abstract</b>	<b>1</b>
<b>1. Introduction</b>	<b>2</b>
<b>2. Considerations in the Design of the Specimen</b>	<b>5</b>
<b>3. Considerations in the Design of the Test Set-Up</b>	<b>9</b>
<b>4. Results of the Test Program</b>	<b>13</b>
<b>5. Test Data Management</b>	<b>18</b>
<b>6. Computer Modeling</b>	<b>23</b>
<b>7. Discussion of Results</b>	<b>26</b>
<b>8. Conclusions</b>	<b>37</b>
<b>References</b>	<b>40</b>
<b>Appendix A. Tables &amp; Figures</b>	<b>41</b>
<b>Vita</b>	<b>75</b>

# List of Figures

<b>Figure A-1:</b>	Typical Connection Detail	44
<b>Figure A-2:</b>	Type 1 Connection Detail	45
<b>Figure A-3:</b>	Type 2 Connection Detail	46
<b>Figure A-4:</b>	Reaction Frame & Test Setup	47
<b>Figure A-5:</b>	Instrumentations for Tests	48
<b>Figure A-6:</b>	Loading Sequence for Test 1	49
<b>Figure A-7:</b>	Loading Sequence for Test 2	50
<b>Figure A-8:</b>	Loading Sequence for Test 3	51
<b>Figure A-9:</b>	Load-Deflection for Test 2	52
<b>Figure A-10:</b>	Load-Deflection for Test 3	53
<b>Figure A-11:</b>	STRUCTR Model for Connection Members	54
<b>Figure A-12:</b>	Exploded Force Diagram for Connection Members	55
<b>Figure A-13:</b>	Bolt Slip at Edges of Web Plate	56
<b>Figure A-14:</b>	Fixed End Beam Supports for Top Flange Plate	57
<b>Figure A-15:</b>	Simple Span Bending of Top Flange Plate	58
<b>Figure A-16:</b>	Deflection at Column Flange Tips	59
<b>Figure A-17:</b>	Shear Stress Between Rosettes 12 & 15	60
<b>Figure A-18:</b>	Shear Stress Between Rosettes 1 & 2	61
<b>Figure A-19:</b>	Shear Stress Between Rosettes 5 & 6	62
<b>Figure A-20:</b>	Shear Stress Between Rosettes 8 & 9	63
<b>Figure A-21:</b>	Bending Stress Between Rosettes 1 & 2	64
<b>Figure A-22:</b>	Bending Stress Between Rosettes 8 & 9	65
<b>Figure A-23:</b>	Stress Flow from Web to Flanges	66
<b>Figure A-24:</b>	Rosette Location of Bottom Flange	67
<b>Figure A-25:</b>	Bending Stress Between Rosettes 20 & 29	68
<b>Figure A-26:</b>	Integration of Rosettes for Web Shear	69
<b>Figure A-27:</b>	Shear Stress Distribution in Beam Web	70
<b>Figure A-28:</b>	Through-Thickness Restraint on Welds	71
<b>Figure A-29:</b>	Rosette Location on Top Flange	72
<b>Figure A-30:</b>	Rosette Location on Beam Web	73
<b>Figure A-31:</b>	Proposed Suggestions for Improvement	74

## List of Tables

<b>Table A-1:</b>	Comparison of STRUCTR and Test Results	42
<b>Table A-2:</b>	Comparison of Stresses for R1 & R8	43
<b>Table A-3:</b>	Comparison of STRUCTR with Measured Loads	43

# Abstract

**KEY WORDS:** columns(support);cyclic loading(earthquakes),framed structures,finite element method(analytical model);plasticity;fracture mechanics;welded joints,matrix methods.

Continuation of the beam-to-column research begun at Fritz Engineering Laboratory, Lehigh University simulating the cyclic loading of a beam-to-column weak-axis moment connction. Behavior of this sort is required to determine the acceptability of a fully welded design when subjected to a dynamic loading. Critical factors in the connection detail are the thickness of the connection plate, weld sizes, elimination of a backing stiffener opposite the beam and defects in workmanship. Discussion of previous work on full scale moment connections, considerations in the design of the test set-up and the overall approach to the intent of the testing procedure are expressed. Micro-computer based data reduction programs are implemented to retrieve and graphically display the data. Theoretical studies are presented as a means to relate empirical results to matrix structural design methods to be considered in future building codes. Presentation of experimental results concerning ultimate load and ductility for two types of welded details with conclusions regarding areas for future study.

**REFERENCE:** Heaton, Kenneth A., "Cyclic Behavior of Beam-to-Column Weak-Axis Moment Connections," Master's Thesis, Lehigh Univ., May, 1987.



# Chapter 1

## Introduction

Over the past forty years a series of research projects on the subject of beam-to-column connections were conducted in the Fritz Engineering Laboratory at Lehigh University. Previous work included riveted connections, semi-rigid connections, flexible welded angle connections, subassemblages representing a portion of a structure, and beam-to-column web connections. Tests conducted by Rentschler and Driscoll on beam-to-column web moment connections subjected to a statically applied bending moment raised concern about the safety of such connections under a dynamic loading condition [8]. In one of these tests, failure of a fully welded moment connection was due to an instantaneous break across the entire tension flange near the welded zone when the applied load reached 85% of the plastic moment. Clearly this does not indicate good ductile behavior. Results by Popov [6] on a similar but smaller member subjected to cyclic loading demonstrated a brittle type fracture that was also unsatisfactory.

Poor results could be traced to a combination of causes such as the geometry of the connection, location of the groove weld and defects in the welding procedure or workmanship. These parameters were examined in a series of reports by Pourbohloul [7]. Variables of these tests were the connection plate geometry, plate thickness, weld size and the use of a backup stiffener. Results of these tests improved the knowledge of the failure mode of column connections so that design recommendations were made to direct the course of further study.

The current investigation was conducted under Fritz Engineering Laboratory Project 504 funded by National Science Foundation Grant No. ECE-8320540. The grant was for a program including theoretical studies and full-scale tests on weak-axis beam-to-column moment connection details [5]. Test setup design began in September 1985, fabrication of the components was done in February thru May of 1986 and testing was conducted during the months of June thru November of 1986. Originally, the project was to include two tests, but due to a premature weld failure in the first test it was possible to repair the specimen and retest it for a total of three tests.

The intent of the project was to simulate a single-sided beam subassemblage as would be found on the exterior of a building. See fig. A-1. The test specimen was restrained in a large fixture, and loading was applied at the tip of a cantilever arm in cyclic load steps. Each cycle consisted of both positive and negative vertical deflection increments. The program for the load steps will be discussed further in the testing section.

Two types of connections were tested. The main points of Type 1 were:

- 1.) No backup stiffener
- 2.) Fully welded around beam flange connection  
plate to column web and flanges
- 3.) Bolted web connection
- 4.) Beam flange connection plate extended past column  
flange tips

The Type 2 connection detail differed from the above in that the beam flange

connection plate was not welded to the column web, and the beam flange connection plate was increased in thickness to account for the full-span effect between the column flanges. See fig. A-2 & A-3 for design details of Type 1 & 2.

The significance of this test is that only a limited number of weak-axis beam-to-column moment connections have been tested under cyclic loading conditions. The members tested here are larger than any previous cyclic loading test of this type. There are some effects of size that can not be scaled up, they can only be determined experimentally. Once the phenomenon that has occurred in the full-scale test is understood then a model can be developed to predict future behavior. Guidelines must be established to insure the safety of large-scale fabrications so they can withstand severe loading conditions such as an earthquake.

Attention was focused on the details of the welding procedure, weld location and size, thickness of the connection plate members, and number and location of the bolts in the web plate joint. A balance between member size, ultimate strength, and ductility must be achieved in order to maintain structural integrity during large distortions into the inelastic range.

## Chapter 2

# Considerations in the Design of the Specimen

In order to maintain continuity with the earlier work of Rentschler [8] on full scale connection tests and the flange connection plate detail tests of Pourbohloul, et. al. [7], a W27 x 94 beam and two columns, a W14 x 174 and W14 x 257 were selected as typical members in a building frame. Primary components that must be designed are:

- 1.) Beam flange connection plate
- 2.) Beam web connection plate
- 3.) Welds of connection plate to column
- 4.) Full penetration weld between the beam  
flange and the connection plate.
- 5.) Location, number and size of bolts in  
web joint.

Each of these items will be discussed below:

Item 1: The thickness of the beam flange connection plate for the Type 1 & 2 connections was determined by the previous work of Pourbohloul [7]. The plate was extended three inches past the column flange tips in order to reduce the stress concentration at the re-entrant corner. The plate was tapered in the thickness direction at a slope of 1:2.5 in accordance with the Structural Welding Code [2] fig. 8.10A for butt joints in parts of unequal thickness and offset alignment. The plate was not tapered in the width direction. However, the amount of extension provided was sufficient to permit the path of tension

stresses to flow at an angle of 45 degrees from the column flange tips to the edges of the beam flange as recommended by Pourbohloul [7]. Plate thickness and the lack of welds between the column web and the connection plate were the only differences between Type 1 & 2.

Item 2: The beam web connection plate was sized to be 9/16 inch in the thickness direction, but obtaining plate this size was difficult so the thickness of the web plate was increased to 5/8 inch to allow delivery of a stock item. Care was taken to allow a generous radius at the cut out portions of the plate.

Item 3: Weld sizes were originally designed on the basis of the maximum static loads to resist the shear and bending moment components of the applied vertical load. This was shown to be inadequate in Test 1 because the Poisson's ratio effect produced through-thickness stresses that caused cracks to develop at the root of the weld. A detailed description of the through-thickness effect will be given in the discussion of results. These welds were double fillet all around the edges of the plate except the column web weld was eliminated in the Type 2 connection, Test 3.

Item 4: The full penetration weld between the beam flange and the connection plate was per the ANSI/AWS D1.1-86 code, fig 2.9.1 for single bevel groove weld butt joint with backing bar [2]. This weld was dye-checked and ultrasonically tested for the first test. The backing bars were removed and any irregularities ground down and repaired. This procedure was done to reduce the problems due to stress concentrations cited in the work of Pourbohloul [7]. Further comments will be made in the discussion of results.

Item 5: Seven one-inch A490 bolts were used in the design to carry the vertical shear load, but it was not possible to design a single row of bolts to develop the entire plastic capacity of the beam web. This meant that the beam flange connection plate had to accept higher normal forces due to the reduced capacity of the web plate. (Later work by Lu tested the ultimate capacity of these bolts.)

The specimen was proportioned with the overall length of the cantilever exceeding the distance in which shear load would affect the final failure mode. Fabrication was done in Fritz Lab and the process was closely monitored. Care was taken to orient the rolling direction of the connection plates with the longitudinal axis of the beam. Failure to do this was cited as a problem in earlier testing. Bolt torque was checked by turn-of-the-nut method.

The fabrication quality of the finished specimens was good and probably better than the average field craftsmanship. The welds were of proper size and did not have porosity, surface cracks or inclusions visible to the naked eye. Ultrasonic examination of the groove weld revealed some small voids and/or inclusions but these were not large enough to require repairing the welds. These inclusions were documented. Comments regarding the fracture mechanics approach to the weld failure will be made later. A heavy mill scale on the surface of the connection plate may have affected the depth of penetration and this will be discussed in the results section.

Additional aspects of the specimen designs were based on results of other

investigations. A properly designed and fabricated connection will exhibit ductile behavior and failure away from the groove weld of the connection plate to beam flange joint. Popov reached some fundamental conclusions as to the result of his work. The load deflection hysteresis loops for a steel cantilever beam and connection are highly reproducible during repetitive load application. This fact implies that such an assemblage is very reliable and can be counted upon to absorb a definite amount of energy in each cycle for a prescribed displacement. The ability to withstand severe repeated and reversed loading seems to be assured for properly designed and fabricated steel structures; their intrinsic energy absorption capacity is large [6]. This energy absorption capacity, as measured by the size of the hysteresis loops, increases with increasing tip deflection until the maximum loop outline is reached.

These assumptions form the basis for comparison of test results for different connection details. Some sort of standard must be established as a guideline for an acceptable connection design. The ultimate energy absorption capacity of the test detail must be compared to this standard to determine if it meets the minimum requirements. For this series of tests the standard was chosen at three cycles where the load reached positive plastic moment and negative plastic moment based on recommendations by a European committee [9].

## Chapter 3

### Considerations in the Design of the Test Set-Up

As stated above, this test was unique in that full size members were cyclically loaded to plastic bending failure. Due to the magnitude and application rate of the forces required to cause failure, careful design of the reaction frame was mandatory. Unfortunately, space constraints on the testing floor and availability of testing frame members restricted the reaction frame to less than optimum design. The frame used for this test was essentially a two-dimensional structure with the cantilever beam, column and loading mechanism in the plane of the reaction frame. See fig. A-4. This greatly reduced the width of the frame allowing it to be erected in a small corner of the lab, but it did not allow for cross-bracing. A forty-five degree leg braced one corner only, while lateral struts stabilized the frame to the building wall. The entire frame was bolted together so that it could be taken apart to change the test specimen.

The loading forces and reactions were modeled using STRUCTR--a Structural Analysis Program developed by Driscoll and students at Lehigh University [4]. The program inputs the number of members, joints, type of restraints, member properties and material constants. Using the output from the program, the deflections and forces at all ends of the members can be determined.

Another factor in the design of the test is the loading system for the



beam. Since the test was to simulate dynamic loading conditions as much as possible, hydraulic power was chosen as the prime source for a displacement driven test program. Two hydraulic actuators operating in series (i.e., one in compression the other in tension) were needed to reach the failure load of the specimen and not overload the capacity of the actuators at their extended length. The units used in this test were 8-inch bore by 24-inch stroke T. J. cylinders manufactured by Aero-Quip. Pin connections at both ends of each cylinder allowed displacement of the beam and rotation of the cylinder without binding the piston to the bore. The hydraulic pumping system used was an Amsler swing arm pumping unit which has exceptional flow control and can maintain a steady pumping pressure almost indefinitely. Direction of travel of the actuators was changed by using a Moog servo valve with a remote control at the Amsler control panel. After some initial start-up problems the system performed almost flawlessly.

After the connection details had been designed, the reaction frame built, and the hydraulic system put together, the next major phase and probably the most critical was the acquisition, storage and reduction of the test data. Instrumentation line-up for Test 1 had 31 rosette strain gages, 8 linear gages, 7 dial indicators, 2 linear variable displacement transformers(LVDTs), a load cell, and 2 rotation gages. There were 101 channels of strain readings to be recorded at each load step. Four of the strain gages were wired together in series and read manually by an operator. These four channels were calibrated at a specific point along the length of the beam away from the yield zone to a 50 kip load cell. Using this calibration and extrapolating the load range

(assuming linear behavior) the load could be read versus a prescribed displacement. Subtracting these four gages from the total left 97 remaining channels that had to be recorded. A micro-based data acquisition system was used for this purpose. Unfortunately, the system proved to be the weak link in the operation. Unreliability, problems with the software, disk drive errors, slowness, and limited screen visibility created many headaches. Some file security was achieved by linking the system to an independent micro and transferring data files to its hard disk once or twice a day. Even with this backup, some files were lost. Counting all the delays and breakdowns, at least two weeks were lost during the course of the test.

In addition to the strain gages, the other items of interest had to be recorded manually. Dial gages, LVDTs, load cell readings and various book-keeping information such as load number, date and time had to be written down in specially formatted tables for each load step in the cycle. Some readings such as load and displacement were checked at the beginning and end of each recording cycle to make sure the values had not slipped due to yielding. This was especially critical at displacements in the inelastic range. The entire recording process took three to five minutes (depending on the size and skill of the crew) and to complete one load cycle could take four hours.

See fig. A-5 for the location of the dial gages and LVDTs. Dial gages were used to measure bolt slip at the edges of the web connection plate, the movement of the web connection plate at the center of the column web and the Poisson's effect at the column flange tips where the horizontal connection plates

were located. The LVDTs were used to measure the displacement of the beam tip (this was called the "criterion" measurement since it controlled the test) and the sway at the top and bottom of the column. Column sway was measured to calculate the angular rotation of the column centerline which contributed to the beam tip displacement.

Photographs were taken of the overall test setup and at various stages of interest such as maximum load or fracture of a weldment. As mentioned above, an attempt was made to measure the rotation of the beam with respect to the column using some very old rotation gages but these did not work. Unfortunately, this critical angle of rotation could not be determined reliably.

## Chapter 4

### Results of the Test Program

The programmed loading sequence was applied in increments of load and displacement over a range of cycles that represented a prescribed percentage of the maximum yield load. Each cycle was repeated three times in order to simulate the energy of an earthquake. The peak amplitude of each group of three cycles was chosen to be one fifth, two fifths, three fifths, four fifths and equal to the amplitude required to cause plastic moment. The plan was to work gradually up to the plastic moment and then repeat this cycle three times. If the specimen were still intact then three more cycles of twice the amplitude of the plastic moment were to have been applied. However, as will be seen this procedure was somewhat academic.

Test 1--This test was conducted on the Type 1 connection( see fig. A-2 for details) which was welded along the flange plate connection to column web. The load was applied as described above, see fig. A-6. As shown in the plot the connection failed in the eleventh cycle at load step 158, which was approximately 86% of the required plastic load. Failure was by a sudden fracture of the left fillet weld in the top flange connection plate. The fracture occurred on both the top and bottom fillet welds along the column flange portion of the plate and around the corner through about half of the fillet welds along the column web. The initiation point for the crack appeared to be at the column flange tip and it then worked slowly back along the inside face of the flange when the weld was in tension. When the weld was in compression the crack appeared to close. Fracture mechanics states that when

the crack driving force exceeds the crack resistance strength, unstable growth occurs. As the load was increased to higher levels, the driving force increased as the crack grew and the stress intensity level was raised. Crack growth resistance increases with small increments to crack growth so the resistance was able to keep up with the early stages of crack extension. Ultimate crack growth resistance is a finite material property so when the limit is exceeded there is nothing left to resist fracture; therefore brittle (sudden) failure results.

Failure in this test was at a load about 14 percent less than expected and the major components had undergone little if any yielding. A decision was made to repair the welds and resize them considering the through-thickness effect of Poisson's ratio. This will be discussed in greater detail in Chapter 7. Thus the fractured 13/16 inch fillet welds were burned out and replaced by 1 inch fillet welds. The specimen was put back in the test frame and prepared for testing.

Test 2--The second test on the repaired specimen gave much better results. The connection had adequate strength to develop the full plastic moment of the cantilever beam. There was also adequate ductility to permit three cycles of reversed plastic moment. See fig. A-7 for a plot of the load versus increment number. After completing the program of controlled loading cycles, a final monotonic load cycle was applied in order to determine the maximum deformation capacity of the specimen. Loading in the negative (downward) direction was halted when a crack initiated in the groove weld connecting the beam tension (top) flange to the connection plate. Loading was reversed,

because the crack area could resist compression as the crack closed. Displacement in the reversed (positive) direction was applied until cracking occurred in the fillet welds along the column flange on the lower right hand side. The maximum load reached was about 122% of the calculated plastic moment. The maximum displacements were about +168% and -195% of the observed yield displacement.

Examination of the column flange fillet weld crack showed that it was quite similar to the failure in Test 1. Again the crack appeared to start at the column flange tips, perhaps due to a poor penetration of the root pass in this area. However, this time the fillet welds displayed quite a bit of ductility (yield lines can be seen along the weld surface) and held together for large strain rates.

The crack in the tension flange full penetration weld can be shown to be initiated by an elliptical flaw in the middle of the weld zone. The presence of this flaw generates a high stress field around the perimeter of its boundary, these high stresses produce localized cleavage failure. This can be seen as areas of flat fracture. As the crack progresses along the width of the beam flange its mode of failure becomes slanted indicating a more ductile or shear failure. The initial flaw may have required several cycles to grow large enough to induce a critical stress field but once it reached this limit the growth became unstable.

Test 3--The third test was conducted on the Type 2 specimen (see fig.

A-3) in which the fillet weld along the column to the top and bottom connection plates was eliminated. This had the effect of creating a bridge between the inside faces of the column flange, making the welds along this area even more critical. For this test a heavier column section, a W14 x 257 was used. The planned loading sequence was applied. See fig. A-8 for a plot versus load number. As can be seen from this plot, the connection detail was able to achieve the theoretical plastic moment in both the positive and negative direction. The goal of three cycles at plus or minus plastic moment was not met, so the Type 2 connection did not meet the full ductility requirement.

Again cracks were seen to initiate in a fillet weld along the column flange, this time it was the lower left corner weld. The crack was observed to grow when the connection plate was held in tension. During the start of the third cycle of the plastic moment loading sequence the crack fractured suddenly. The results were mixed: the desired load was achieved, but the ductility was not acceptable.

In reality the ultimate plastic moment was not reached in this test either. This can be seen by comparing the load versus deflection curves for Test 3 with Test 2. See fig. A-9 and A-10. In Test 2, the curve "flattens out" as the ultimate plastic moment is approached, in Test 3 the curve is still climbing as can be seen by the relatively steep slope. The theoretical plastic moment was achieved in Test 3 but this is calculated based on a yield strength of 50.0 ksi. The beams used in these tests had a yield strength of 58.0 to 60.0 ksi hence the ultimate load should be higher than the theoretical by about 20 percent. This

goal was reached in Test 2 as the ultimate load was about 22 percent higher than the value calculated using a yield stress of 50.0 ksi. The ultimate value was higher than the value calculated using a yield stress of 60.0 ksi even though yielding had not progressed through the entire beam web. It is doubtful that a moment connection with a bolted web joint will ever develop the full plastic moment simply because of the high strain rates required to plastify the web. Something usually fractures in the top flange connection plate assemblage before the plastic zone extends completely through the web.



## Chapter 5

# Test Data Management

As discussed previously, each of the three tests generated huge volumes of data. In the past, the general procedure is to use existing software on the data acquisition system to calculate the desired stress-strain results. This can be done on certain systems. The software for these machines is somewhat limited and their fixed output format makes application of some other post-processing device difficult, i.e., if one wishes to obtain plots of various stress results.

A different strategy was used for this project. A micro with a hard drive disk was connected to the data system via an RS 232 port running an interfacing program. This hook-up allowed data file transmission of the automatically recorded results to an independent hard drive for later post-processing. This streamlined the data reduction effort while adding much needed file security to backup the delicate dedicated disk drive. It was no longer necessary to run the built-in stress-strain processing software and view a paper printout. Once the raw data files were on the hard disk they could be neatly copied to floppy disks for convenient storage and transportation.

The raw files had to be reduced and grouped according to the strain rosettes or linear gages that corresponded to the actual channels read. Also, there were 13 or 15 manual readings for each load step of each test. These manual readings had to be combined with the automatic readings taken at the same time. A scheme was devised to do this using a micro running a Basic language program. Three programs were used to reduce, collect and combine all

the information for a particular load step. First, program DATIN took a raw data file and compressed it into a format that could be combined with the manual data. This program removed all the headings, titles, page numbers, etc. that were present in the formatted printout of raw data and converted them to a list of channel numbers and the corresponding strain at each load step. Second, a program called MANIN was used to input the manual data at each load step. The program prompted the user for the given manual reading, i.e., Dial Gage No 1 or LVDT No 2 etc. for each load step which was then written to a file for the manual data. Each file consisted of ten to fifteen load steps; care was taken to match the starting and ending number with the corresponding number for the raw data file from the data acquisition system. Test 1 had 159 load steps, Test 2 had 194 load steps, and Test 3 had 239 load steps. One can easily see that many data files were generated and record keeping was very important.

The third program was COMDAT and logically enough this program combined the compressed electronic data file with the corresponding manual data file. In this manner, all the raw data records for each load step were consolidated in a single list. All this sounds very simple but considering all the little mix-ups and acquisition system operating problems the above operation took months.

Once all the data files were generated the actual post-processing could begin. The scheme behind the data processing was this:

1. Input a setup file with test parameters describing location of gages,

channel numbers, material properties and desired items to be calculated.

2. Take all raw data stored and subtract the zero reading to get the difference.
3. Take the difference readings required for a particular rosette/linear gage and transfer them to a subroutine to calculate the stress-strain relationships.
4. Repeat step 3. for manual data
5. Store the load number, date and time at the head of a data file created for each load step. Then store the differences for strain and manual readings. Then store the calculated results, the linear stress results and last store the calculated results for each manual reading.

For each load step there were approximately 400 items (depending on the number of rosettes per test) to be stored. This was done by opening a direct access file and writing the list of items to it for each individual load step. The program that did all this was called DPROC. The program could be run on a micro with 640 K of central memory.

The key point of the direct access system is that now all the results are stored at a particular location in a direct access file. Any result can be

retrieved by another program designed to select a location in the first load step stored and then proceeding to the same location in the next load step. This can be achieved by setting the file pointer to a pre-calculated value depending on the result desired and simply incrementing this pointer value by the number of records stored in each load step. The number of records is a preset constant and this value is added to the initial pointer value for each load step until the file has been read to the end. The desired result is then stored in a temporary array for viewing purposes.

In this manner, a stress value at a particular location on the specimen can be collected for each load step of the test. Once these values have been collected in an array they can be plotted on the screen of the micro-computer using a graphics subroutine. Any desired value can be displayed. For added flexibility a value could be plotted as an ordinate with the abscissa the load step number or the value could be plotted on the abscissa with the ordinate being the load value in kips (eg. load versus displacement). The program that did this was called DPLOT. Once the graph has been displayed on the screen the viewer has the option to create a file for an X-Y plot. This file can be sent to a plotter for hard copy. The plotting software used for this research project was the AUTO\_GRAPH [3] program on the CAE lab mini-computer at the Fritz Engineering Laboratory. This program creates high quality plots and allows the user to plot multiple functions, i.e., two stress results can be displayed on the same plot. A Hewlett Packard pen plotter was used for all the plots found in this thesis.

The two post processing programs and the data reduction programs were written and developed by Dr. George C. Driscoll and students at Lehigh University. The use of these programs on the micro-computer provided tremendous flexibility and power in the data reduction which allowed an in-depth study of the experimental data.

## Chapter 6

# Computer Modeling

The popular technique in computer modeling the past several years has been the finite element method, FEM, using one of the package programs such as SAPIV, ADINA, ANSYS or some other program in vogue. As is common knowledge, this method discretizes the structure as a series of small elements. The number of elements is limited more or less by the size of the computer. But really, the program is limited by the patience of the programmer. In order to make an accurate analysis, one must use more and more elements. Hence the model builder tends to limit the size of his model by making assumptions or restricting the model to a two-dimensional plane. What one generally achieves is a very detailed analysis of a small portion of the original structure. Even with this approach, FEM generates more data than the average engineer can interpret. A worse effect is that one tends to overlook behavior caused by the three-dimensional loading of a structure. Important loads, stresses and reactions are often overlooked by a simplified model.

The intent of this research project was to use a more approximate analysis technique, matrix analysis, but use a more complete three-dimensional model. In this manner, the entire structure could be represented and analyzed using the direct stiffness method program STRUCTR. Some modifications to the program were necessary for the application to this connection detail. STRUCTR is generally used for the analysis of large span structures, i.e., bridges, building frames, truss members, etc. where the length-to-depth ratio is large. This implies that the major component of the element stiffness matrix is distortion

due to bending(flexure). In a beam-to-column connection fabrication, the length-to-depth ratio of the members is about one or less. Shear distortions account for a large percentage of the overall element distortions. The program STRUCTR was modified to include the shear distortions in the element stiffness matrix. The revised program was called STRSHR.

The development of the model was actually simple. Moment of inertia section properties were calculated for bending flexure about the strong and weak axis of each connection plate member and a portion of the column web. Effective shear area was calculated for shear distortions and polar moment of inertia for a thin rectangle was calculated for torsional rigidity. Section properties for the W27 X 94 beam were found in the AISC handbook [1]. The column web was modeled as two separate fixed end beams to include the noticeable deflection of the centerline of the column web at the intersection of the beam web connection plate. See fig. A-11 for a layout of the model. Members 1 & 2 and 3 & 4 represent the column web with points 1, 3, 16, and 18 being fixed restraints provided by the heavy column flanges. Members 5 & 6 and 7 & 8 represent the bottom and top connection plates respectively. Members 9 & 10 represent the horizontal connection plate and members 12 & 13 represent the vertical connection plate. Points 4, 6, 10, 19 and 21 are fixed supports provided by the column flanges. Member 11 is the cantilever beam with the load at point 14. Members 14 thru 25 are dummy rigid members with very high section properties to transfer reactions from one active member to another while maintaining geometric relationships between the members. Joints 7 and 22 are pinned allowing Z axis rotation because no relative

moment can be transferred through the weld. It is assumed that the weld joint transfers only axial force and vertical shear. Joints 9 & 15 are also pinned about the global Z axis. Joint 9 represents the center bolt of the lower group of three bolts while joint 15 represents the center bolt of the upper group of three bolts. This was done to provide an average moment caused by the leverage between the upper group of bolts and the lower group of bolts on the web connection plate.

The model included twenty five elements and twenty three node points, but it fully described the three-dimensional nature of the connection providing a valuable insight into the distribution of the member forces and external reactions for design purposes. An exploded force diagram illustrates this point (see fig. A-12). Traditionally, connections are designed assuming that the vertical web carries all the shear force and the horizontal beam connection plates carry only normal bending stresses uniaxial to the direction of the beam. Examination of fig. A-12 shows that less than 50% of the vertical shear is carried by the web plate and a secondary moment is carried by the top and bottom connection plates due to the component of the vertical shear that is transferred into these members. Thus, even a simple model such as this one provides new information regarding the force distribution in the connection members. The model does have limitations in that stresses due to the through-thickness effects of Poisson's ratio are not included. A comparison of the model to the actual stress distribution will be discussed in the next chapter.



## Chapter 7

### Discussion of Results

This project was unique in that the theoretical analysis was limited, using only a matrix analysis program to solve a simple geometrical model. On the other hand the the amount of data collected and assimilated for computer based retrieval was voluminous. The key to making sense of the data recorded was knowing what to look for and then spot this trend while interpreting the data. Probably over a hundred stress versus load value or number plots were made in order to achieve the few simple observations that will be put forth.

Bolt slip is one of the primary causes for redistribution of the forces in the connection plate members. Bolt slip begins immediately upon application of the first load cycle and parallels the direction and magnitude of the applied load. See fig. A-13. As the flanges begin to yield due to plastic flow the bolt slip becomes at least ten times greater than the elastic range value. A thorough discussion of the consequences of this behavior will be given later. The top and bottom flange connection plates are subjected to bending about the global X and Y axes. Bending about the X axis (YZ plane) approximates the shape of a fixed end beam with a single concentrated load at the center span. The plate is bent in reverse curvature as the heavy fillet welds on each end truly act as fixed supports. This behavior was noticed when analyzing the rosette results in this plane. See fig. A-14. It can be clearly seen that the stress at the exterior rosettes must be opposite in sign to the center rosette gage because the exterior rosettes are outside the center zone defined by inflection points a and b. Although this is a rather simple and straightforward

observation, it took some time to deduce. First the normal stress in the global Z direction had to be interpolated to the neutral axis of the XZ plane bending so the normal stress caused by Y axis bending would not influence the X axis bending stress. Then it was observed that the Z direction normal stress reversed sign between points 1 & 2 and 2 & 3. Finally, the relative proportions of the stresses were of such a ratio as to suggest fixed end conditions. This makes sense when considering the top flange as a thin plate member with a length-to-depth ratio of about eight to one. The heavy 1-1/8 inch double fillet welds act to restrain rotation of the plate ends creating a truly fixed condition.

A comparison of the stress distribution with those predicted by STRUCTR is shown in Table A-1. If one considers only the length of the top connection plate that is restrained by the fillet weld to be effective in development of X axis bending stress, then the moment of inertia at the column flange junction is reduced by a factor of 7/13.80 (length of weld/width of plate). This has the effect of increasing the bending stress at this point by a factor of 1.40. This helps bring the predicted stress more in line with the actual stress along the column flanges. Another factor to be considered is the through-thickness effect due to Poisson's ratio. This subject has been examined in a series of reports by Pourbohloul [7] and these stresses could be superimposed on the results of STRUCTR. Finally, the shear stress distribution assumed by STRUCTR in the web connection plate underestimates the actual vertical reaction in the center of the flange plate. This probably accounts for the fact that the measured bending stress in the flange plates is higher than the predicted value.

Bending about the Z axis (XY plane) more closely approximates single curvature beam bending with a distributed load over a central portion. See fig. A-15. This was deduced by observing that the Z directed normal stress always maintained a gradient of the same sign for a given loading direction between rosettes R12 & R15, R13 & R16, and R14 & R17 which implies a simple beam deflected shape with pinned ends. See fig. A-29 for location of rosettes. This can be supported by observing the relative deflection of the tips of the column flanges. See fig. A-16. This plot shows that the column flange tips move in and out in phase with the applied load (ie. as the load is applied upward the beam action pushes the top column flange out and pulls the bottom flange in). Another reason for supporting the single curvature hypothesis is the fact that the horizontal connection plates are not welded along their entire length so there is no restraint over a portion of their cross section.

The input to STRUCTR was modified to account for the single curvature bending effect of the horizontal flanges by releasing the global Y rotation at the node points representing the column flange attachment points. This was done at node points 4, 6, 19 and 21 on the connection model. The revised connection model was called Model II and had the effect of increasing the stress closer to levels measured. Members 14 and 17 were also changed to simple truss members so they would transmit no bending to the column web. This more closely approximates the actual condition since the top and bottom connection plates are not welded to the column web.

An interesting comparison can be made between the measured XY shear

stress with that predicted by STRUCTR results on the top flange, see fig. A-17. The shear stress is plotted at R12 & R15 versus length along the flange. The shear stress is assumed to increase over the constant thickness portion of the plate and remain constant as this plate decreases in thickness. Integrating this stress over the length of the plate gives a resultant shear load for this plate element. Comparing the STRUCTR prediction at Load Step 146 ( $P = 125.0$  kips) which gives a horizontal shear resultant of 172.8 kips versus the resultant by integration of 182.9 kips yields an difference of 10.1 kips or 5.5%. Finally, a comparison of the column centerline deflections shows that the values predicted by STRUCTR at high load steps were within  $\pm 0.005$  inch to those recorded. The measured value was 0.010 inch versus 0.014 inch predicted.

As stated previously, the traditional assumption regarding the distribution of shear stress in the beam web does not apply in the vicinity of the bolted joint. The bolted joint between the beam web and the vertical connection plate fails to transmit 100% of the vertical shear and bending stress in the web section. This is due to the bolt slip that occurs immediately on cyclic loading. See fig. A-18, A-19, and A-20 for a comparison of shear stress between rosettes R1 & R2, R5 & R6, and R8 & R9. This clearly shows that the upper and lower pairs of rosettes, R1 & R2 and R5 & R6 respectively, are influenced dramatically by this slip action while the center pair, R5 & R6, show relatively equal values. This is expected because there is no bolt slip at the level of the neutral axis. See fig. A-30 for a location of the rosettes in the web section.

One can see the dramatic drop in normal stress due to the slip action

looking at the normal stress distribution. See fig. A-21 and A-22 that show a comparison of X direction normal stress for rosettes R1 & R2 and R8 & R9. No appreciable stress is transferred until the strain becomes so large that the bolts actually "bottom out" in their holes. It can be seen that once a bolt becomes locked in one direction it can resist no load in the other direction. If the strain rate in the other direction were so great that it caused the bolt to travel the entire clearance tolerance to lock up on the opposite side, only then would it be able to develop any force in this direction. The unresisted normal stress and the percentage of web shear not transferred through the bolts must flow to the connection plate flanges. A review of the angle to the principal stress for R1 and R8 shows this effect (see fig. A-23).

Another interesting effect is an unequal distribution of bending normal and shear stress about the neutral axis for higher load levels. Elementary beam theory states that these stresses should be equal but opposite for bending stress and equal for shear stress at the same distance above and below the neutral axis of the member. See Table A-2 for a comparison of these stresses between rosettes R1 and R8 which are both 9 inches from the neutral axis. The stresses for rosette R1 are significantly higher. See fig. A-24 for a location of the rosettes on the bottom flange.

The top flange attracts more bending stress which consequently raises the stress level in the upper half of the beam. A hypothesis which deals with the geometry of the flange connection plates will be presented to explain this phenomenon. The top connection plate is about one inch higher than the top

beam flange while the lower beam connection plate is flush with the bottom side of the beam flange. This has the effect of making the connection plate assemblage stiffer above the beam neutral axis than below (the beam neutral axis is below the neutral axis of the connection plate). The resultant normal stress in the beam is thus slightly higher on the upper side than the lower side. Looking at Table A-2 the bending stress at R1 is greater than R8 for loads 15, 57, 106 and 155. The measured stress brackets the calculated stress values for loads 15 and 57. At load 106 the top flange is very near yield and the calculated stress is slightly greater than the measured. See fig. A-25 which shows a comparison of stress at R20 of the top flange and R29 of the bottom flange. At load step 155 the top flange has yielded and the stress at R1 is still greater than R8 but now less than calculated. At load step 214, both flanges have yielded and the bending stresses are about equal, but much less than calculated.

This behavior shows how the bending stress redistributes itself in the web due to yielding and bolt capacity. At high strain rates approaching the plastic moment of the beam, the bolts have reached their maximum capacity to carry load and the bending stress in the web becomes equalized between the top and bottom halves. Once this limit has been reached the additional amount of stress that would normally be carried in the web by a welded joint must be transferred to the beam flanges. This hypothesis violates the plane sections remain plane assumption of simple beam theory and St. Venant's principle does not apply.

In comparing the measured shear stress with the calculated shear stress, the value measured at R1 is again higher than R8 for load steps 15, 57, 106 and 155. The measured values bracket the calculated value at this location. At load step 214, both the top and bottom flanges have yielded and the measured value is greater than the calculated value. The shear stress at R8 is slightly greater than at R1. The measured shear values are greater than required to be in equilibrium with the applied load. This suggests that the yielding action has increased the shear stress above what would normally be expected in simple beam theory.

Next the measured shear stress in the beam web was compared to the value predicted by STRUCTR. A plan was devised to integrate the shear stress over the depth of the web to obtain a vertical resultant which could be compared with the applied load. The shear stress value at a particular rosette was assumed to be the average value for an assigned area. Since the off-center gages are plus or minus nine inches from the beam centerline and the beam is twenty seven inches deep, the effective length for each gage was chosen to be nine inches. This allowed integration along vertical rows of gages: R1, R5 & R8; R2, R6 & R9 and R4, R7 & R11. See fig. A-26 for a general description of the assumed shear stress distribution along the first row of vertical gages, R1, R5 & R8. A simple formula was used to calculate the resultant load:

$$P_{calc} = t \cdot h \cdot (R1 + R5 + R8)$$

where R1 is the shear stress at rosette 1

$t = 0.51$  inch for the beam web

$t = 0.625$  inch for the connection plate

$h = 9.0$  inch

See Table A-3 for a comparison of the load at three locations along the beam and connection plate assemblage. It can be seen that the actual load value is greater just inside the row of bolts than predicted by STRUCTR but this switches at the column flange junction where STRUCTR predicts a value much closer to that actually recorded. This also explains why the measured Z direction bending stress in the top connection plate is greater than predicted. The unresisted vertical shear in the web plate becomes a concentrated load at the center of the top horizontal member. See fig. A-27 for a general plot of the shear stress in the web. Shear decreases as one proceeds from the beam web into the connection plate and over to the column web. The STRUCTR model could possibly be improved by changing the properties for the members that model the vertical connection plate.

Some final comments regarding the beam flange and connection plate junction should be made on the distribution of X direction normal stress in this area. The normal stress was higher on the tips of the beam flanges than the value calculated by simple beam theory while the stress at the centerline was less than this value. This pattern has been observed by past researchers on weak-axis moment connections because the stiffer column flanges attract more



stress than the flexible column web. Also, the normal stress did suffer some effects of eccentricity going from the thinner beam flange to the thicker connection plate. The stress was reduced in magnitude between the two plates but not by as much as it should have been considering the two areas. An effective moment arm could be deduced for the eccentricity effect using the given stress results if it were considered important.

The next important topic to be discussed is welding. Test 1 failed early due to an undersized fillet weld design that did not account for the through-thickness Poisson's effect. When this condition was included in the calculation and the weld repaired, Test 2 gave good results well into the range of ductile behavior. The weld was resized to account for the through-thickness effect by using a three-dimensional vector addition that included longitudinal, horizontal and vertical shear. An overall resultant weld size was calculated that could be divided by the allowable force per unit length of fillet weld to find the required size. For the case of the Type 2 connection used in Test 3 the calculated fillet weld size was almost twice the plate thickness, so an alternative method was used to find the weld size. The throat dimension of the fillet weld was chosen to be one half the plate thickness, giving an effective weld size equal to the plate thickness. Therefore, Test 3 had very large welds but they still failed early before a full ductile cycle could be completed. The problem appears to be more of a weld type than a weld size. Fillet welds are poor welds for any type of cyclic loading because there is always a crack initiation site at the root. The problem is compounded by the direction of the applied load. Extreme tensile forces are applied to the longitudinal direction of the welds through the

connection plate. As this force increases, the Poisson effect tends to contract the plate in the thickness direction which wants to stretch the weld. At the same time, a vertical force in the center of the connection plate wants to rotate the ends of the plate away from the column flanges. Thus to put it literally, the welds are being stretched and pried apart at the same time. See fig. A-28. Yield lines were seen to develop in the weld surface during the test.

This effect is worst at the column flange tips where there is a re-entrant corner. Fracture mechanics predicts the highest stress concentration at this point. In each of the three tests, cracks were seen to initiate at this junction in the load cycles well below the yield load. As each following cycle was applied these cracks spread around the corner and down the length of the weld. Eventually crack growth was unstable and brittle fracture occurred.

The Poisson effect caused through-thickness forces between the roots of the welds, creating a plane strain condition at this joint. This condition has been observed by researchers working on connection details in previous studies. A full penetration weld will negate the Poisson effect because it will allow the weld material to expand and contract with the plate material. A sound full penetration weld will have no "starter" crack to work through the weld material as does a fillet weld and it will resist the effects of plate delamination that can be caused by cyclic loading.

Poor weld preparation may have hastened the destruction but the end result would still be the same. Each of the three tests failed in a different

corner of the beam connection. Metallurgical examination did cite a problem with some heavy mill scale on the base of one of the broken welds which could have caused poor penetration. This may have reduced the ultimate strength of the weld, but since the crack had already grown to such a critical length, brittle failure was unavoidable. Thus the mill scale can not be blamed for the failure mode but only for the final violent action.

## Chapter 8

### Conclusions

This research has resulted in a simplified analysis of the connection, experimental results that correspond favorably with analysis, design recommendations based on the analysis and experimental results, and recommendations for further study.

It has been shown that a simple three-dimensional model was sufficient to analyze the connection assemblage using a direct stiffness method matrix analysis program. The analytical and experimental study was able to provide a description of the significant force distributions in the connection members.

- Biaxial bending stresses in the top and bottom connection plates were caused by a transfer of a vertical shear force component from the beam web.
- These stresses acted upon the double fillet weld on the ends of the plate causing moment about the longitudinal axis of the weld.
- A vertical force component on the fillet welds was also added by the reaction of the vertical shear not carried by the web connection plate; this is about  $0.125 P$  per double fillet weld.
- Shear distortions are not negligible and must be included in the element stiffness matrix for the plate members.

Observations from the experiments resulted in the following conclusions:

- Load capacity of a single row of bolts was shown to be inadequate to transfer the shear and bending stresses from the beam web to the vertical connection plate. This was evident from the start of the test by bolt slippage (applied force being greater than the static friction clamping force) until the very end of the test where the plastic flow in the flanges caused a redistribution of the normal bending stress.

- The previously discussed Poisson effect caused internal stress between the roots of the welds that also should be included in the design calculations.
- The redistributed stress pattern intensified yielding of the top and bottom beam flanges.
- Flexing of the column flanges and web was observed in each of these two connection designs demonstrating the local effects of a high stress concentration on these members.

A data management strategy was incorporated into the test procedure to account for all possible items (automatic or manual) to be recorded, reduced, combined and retrieved for analysis. The micro-computer programs described in this text provided data files that could be viewed using plotting software making a detailed stress analysis feasible.

- The results of the STRUCTR model compare favorably with the overall stress distribution found by experimental strain gage readings except near the bolted joint.
- It was found that the "web carries all the shear" assumption of simple beam theory does not hold up in a fully welded connection detail, as the horizontal plate members carry significant amounts of the vertical shear.

This approximate analysis was shown to be more informative and realistic about the actual stress distribution than many sophisticated finite element method efforts.

Certain contributions to design recommendations may be extracted from the results of this study:

- For large fabrications involving heavy plate members, the combination of horizontal shear, horizontal bending, vertical shear, and vertical bending requires unusually large fillet welds to join the beam flange connection plates to the column.

- One possible recommendation is to use a full penetration bevel weld on the connection plate to the column flange joint (See fig. A-31 ). However, there must be a range of column and beam web sizes where fillet welds can be used to join the horizontal connection plates to the column flanges.
- The fillet weld on the Type 1 connection along the column web will probably be adequate for the small force observed.
- The use of a backup stiffener would decrease the observed flexing of the flanges and web.

Attempts to formulate design recommendations based of this study and the results of prior investigations, reveal the need for some further studies.

- Further study should be conducted to find the range of structural sizes where fillet welds will be adequate to join the connection plate members.
- Additional investigations are required to determine the influence of the backup stiffener on the ultimate strength and ductility of the assemblage.
- One final topic for further study concerns a suggestion to reduce the stress concentration at the re-entrant corner where crack initiation was seen to start. A "fitted" plate (see fig. A-31 ) may spread the stress out over a wider area and convert some of the shear stress along the inside of the column flanges to direct pull or tension on the edges of the column flanges. In terms of fracture mechanics, this may eliminate the mathematical singularity point due to the re-entrant corner.

Large scale beam-to-column connections of the types tested in this research project are often thought of as rigid or fully restrained assemblages. In reality, each connection is a fabrication involving individual plate members with very high section properties about the major axis but significantly reduced properties about the minor axis. When visualized in this light, connections can be designed using fundamental classical methods once the three-dimensional nature of the loading system is fully understood<sub>9</sub> and applied to each component.

## References

- [1] *Manual of Steel Construction, Eighth Edition*  
AISC, Chicago, ILL, 1980.
- [2] American Welding Society.  
*D1.1-86 1986 Structural Welding Code.*  
ANSI/AWS, Miami, FL, 1986.
- [3] Wiedorn, P. G., Seiler, K. W., & Racine, J.  
*Auto\_graph User's Guide*  
CAE Lab, Fritz Lab, Lehigh University, 1986.
- [4] Driscoll, G. C.  
*STRUCTR--STRUCTURAL ANALYSIS PROGRAM.*  
Technical Report C. E. 451, Fritz Lab, Lehigh Univ., Sept., 1981.
- [5] Driscoll, G. C. & Beedle, L. S.  
*RESEARCH PROPOSAL SUBMITTED TO THE NATIONAL SCIENCE  
FOUNDATION--CYCLIC BEHAVIOR OF MOMENT  
CONNECTIONS.*  
Technical Report, Fritz Lab, Lehigh Univ., March, 1984.
- [6] Popov, E. P. & Pinkney, R. B.  
*CYCLIC YIELD REVERSAL IN STEEL BUILDING CONNECTIONS.*  
*Journal of the Structural Division* 95(ST3):327:353, Mar., 1969.
- [7] Pourbohloul, A., Wang, X., & Driscoll, G. C.  
*TESTS ON SIMULATED BEAM TO COLUMN WEB MOMENT  
CONNECTION DETAILS.*  
Technical Report FL 469.7, Fritz Lab, Lehigh Univ., Feb., 1983.
- [8] Rentschler, Glenn P., Chen, Wai F., & Driscoll, George C.  
*TESTS OF BEAM TO COLUMN WEB MOMENT CONNECTIONS.*  
*Journal of the Structural Division* 106(ST5):1005:1022, May, 1980.  
Fritz Lab, Lehigh Univ.
- [9] Plumier, A.  
*Recommended Testing Procedure for Evaluating Earthquake Resistance of  
Structural Elements.*  
Technical Report, University of Liege, Oct., 1983.  
European Convention Tech. Com. 13.

# **Appendix A**

## **Tables & Figures**



Ld. No.	Gage Line	Measured Stress*	Calc. Stress*	1.4x Calc. Stress*	$\sigma_1/\sigma_2$ (-0.525)	$\sigma_3/\sigma_2$ (-0.388)
15	1	-3.352	-2.317	-3.243	-0.502	
15	2	6.677	4.415	---		-0.804
15	3	-5.366	-1.617	-2.264		
21	1	3.100	2.215	3.101	-0.399	
21	2	-7.770	-4.222	---		-0.184
21	3	1.430	1.546	2.165		
57	1	-4.370	-3.120	-4.368	-0.455	
57	2	9.600	5.947	---		-0.661
57	3	-6.343	-2.178	-3.049		
65	1	4.804	3.125	4.375	-0.456	
65	2	-10.099	-5.956	---		-0.416
65	3	4.206	2.181	3.054		
106	1	-6.990	-4.685	-6.559	-0.457	
106	2	15.310	8.930	---		-0.534
106	3	-8.175	-3.270	-4.578		
114	1	6.399	4.680	6.552	-0.449	
114	2	-14.266	-8.920	---		-0.518
114	3	7.392	3.267	4.573		
155	1	-10.360	-6.240	-8.736	-0.486	
155	2	21.327	11.893	---		-0.497
155	3	-10.598	-4.356	-6.098		
163	1	7.698	6.240	8.736	-0.418	
163	2	-18.422	-11.893	---		-0.603
163	3	11.103	4.356	6.098		

Note:

Gage Line 1 connects R12 & R15

Gage Line 2 connects R13 & R16 \*--These values ksi

Gage Line 3 connects R14 & R17

Table A-1: Comparison of STRUCTR and Test Results

Ld. No.	Bending Stress			Shear Stress		
	R1	R8	Calc.	R1	R8	Calc.
15	-11.21	9.97	10.77	-3.68	-2.58	-3.37
57	-15.06	12.12	14.51	-5.19	-3.55	-4.54
106	-20.92	15.49	21.79	-8.54	-5.72	-6.81
155	-24.45	18.60	29.02	-12.72	-8.28	-9.07
214	-22.85	23.82	36.30	-15.38	-16.96	-11.35

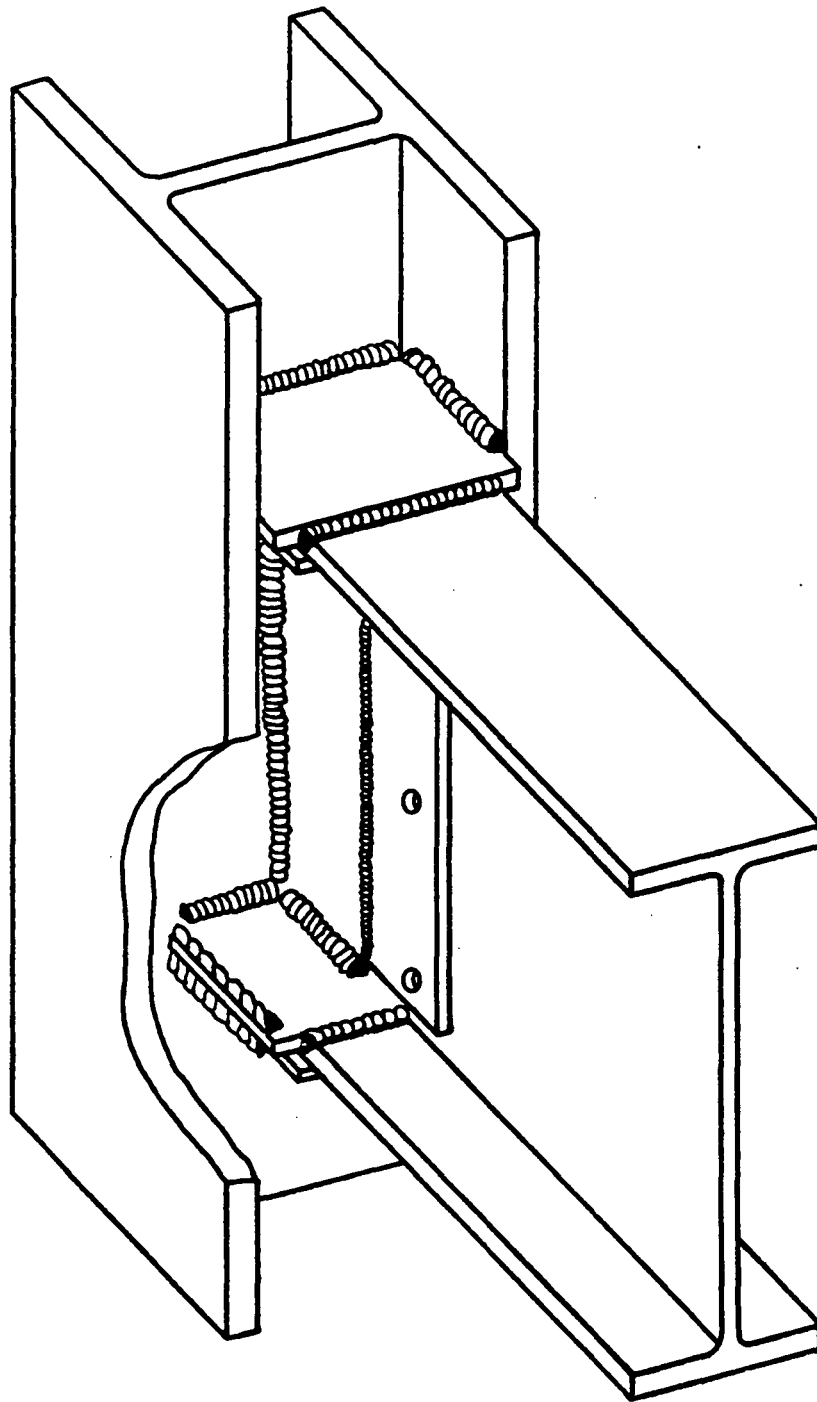
Note: All values ksi

Table A-2: Comparision of Stresses for R1 & R8

Load Number 155  
Applied Load = 125.0 kips

Location	Measured Load (kips)	STRUCTR Prediction (kips)
Beam Web (R1, R5 & R8)	119.0	125.0
Bolted Joint (R2, R6 & R9)	88.2	38.8
Near Column Web (R4, R7 & R11)	51.8	60.0

Table A-3: Comparison of STRUCTR with Measured Loads



**Figure A-1:** Typical Connection Detail

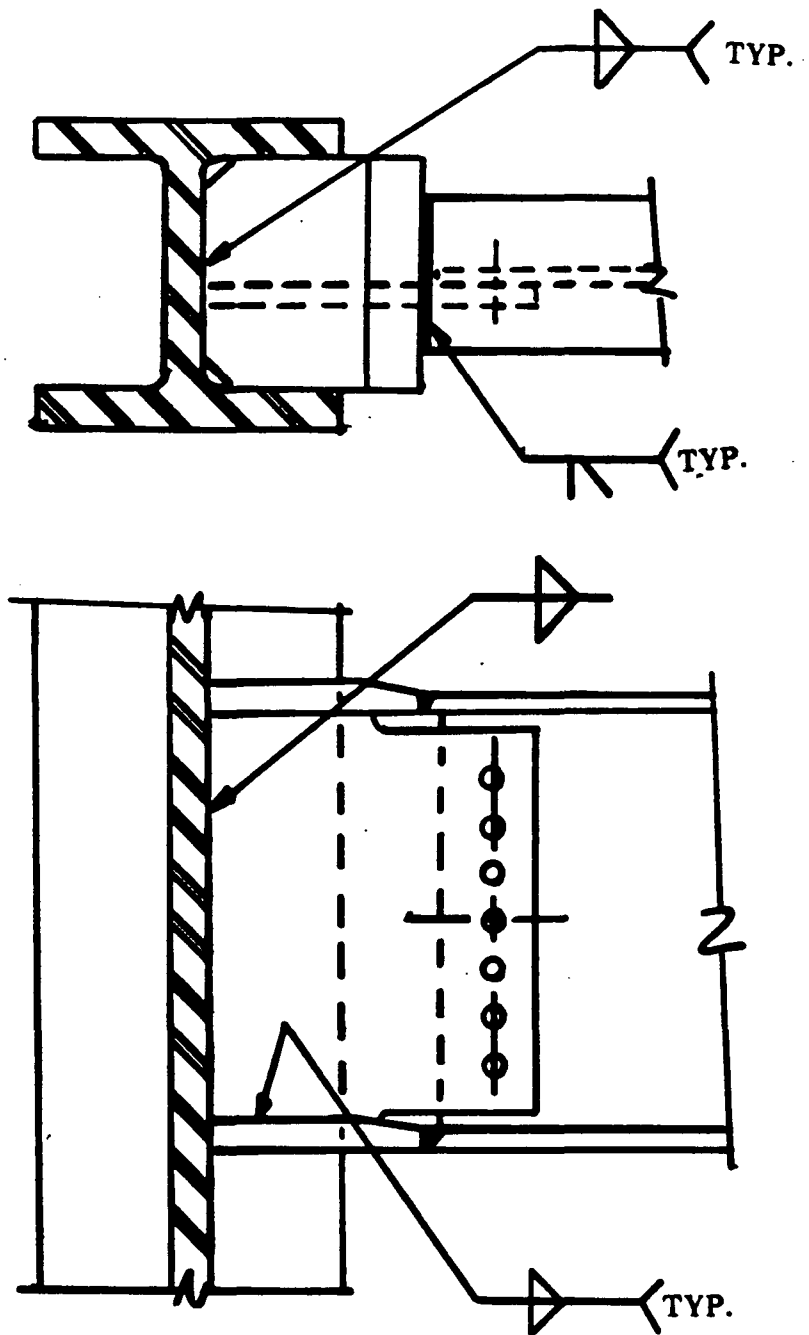


Figure A-2: Type 1 Connection Detail

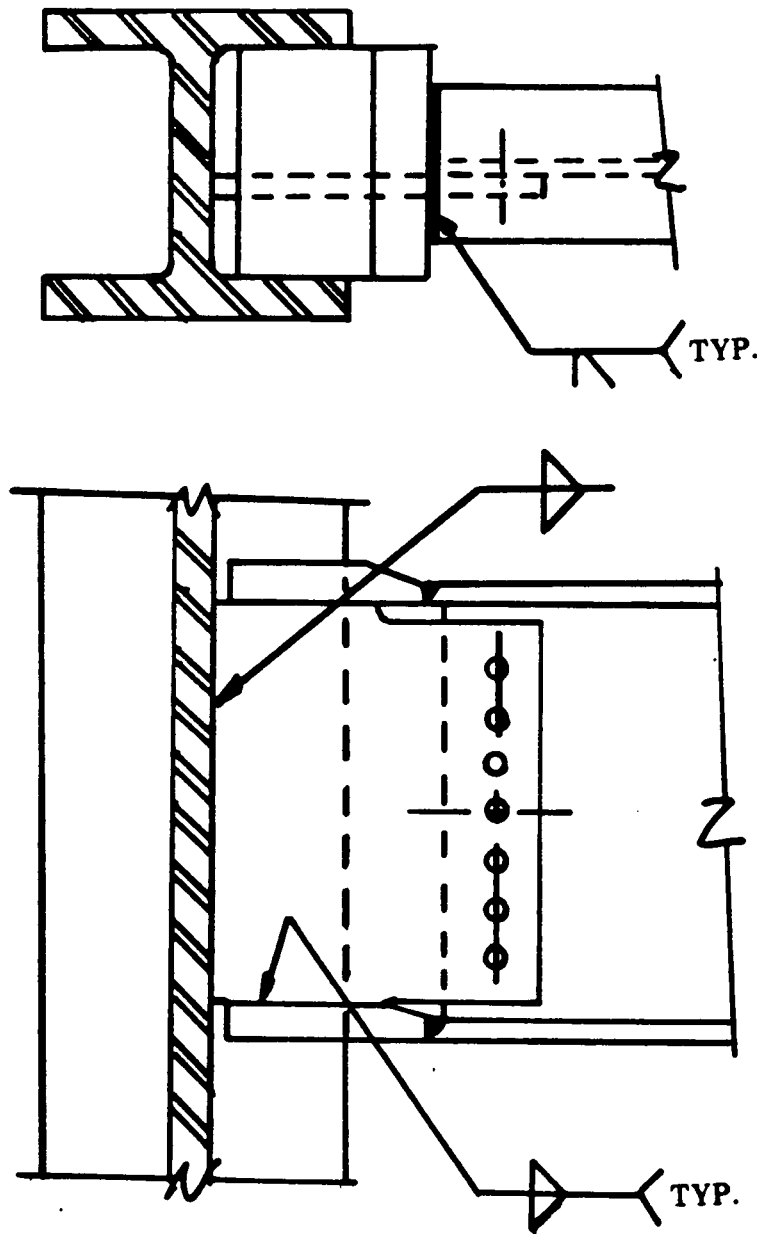


Figure A-3: Type 2 Connection Detail



Figure A-4: Reaction Frame & Test Setup

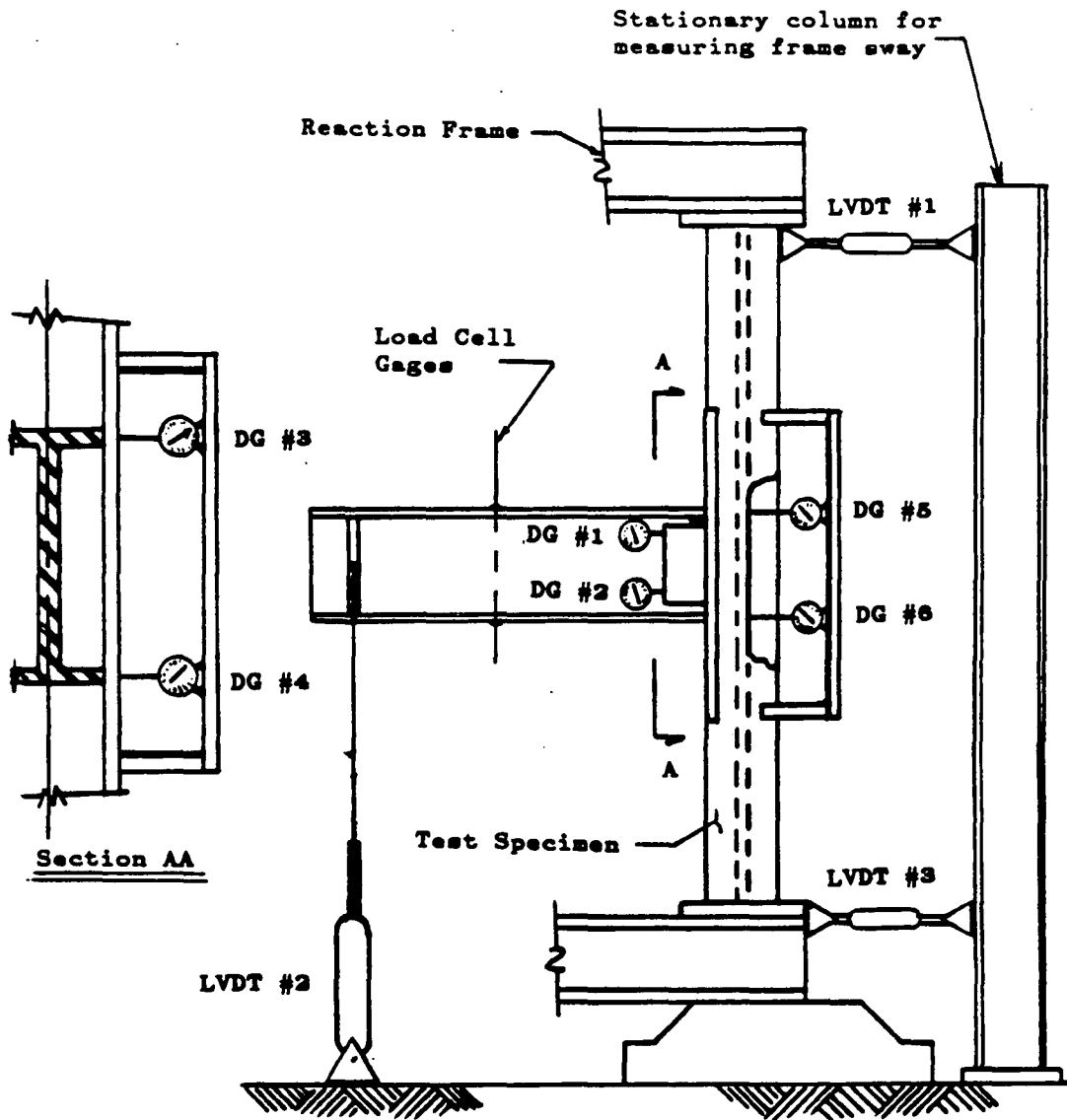
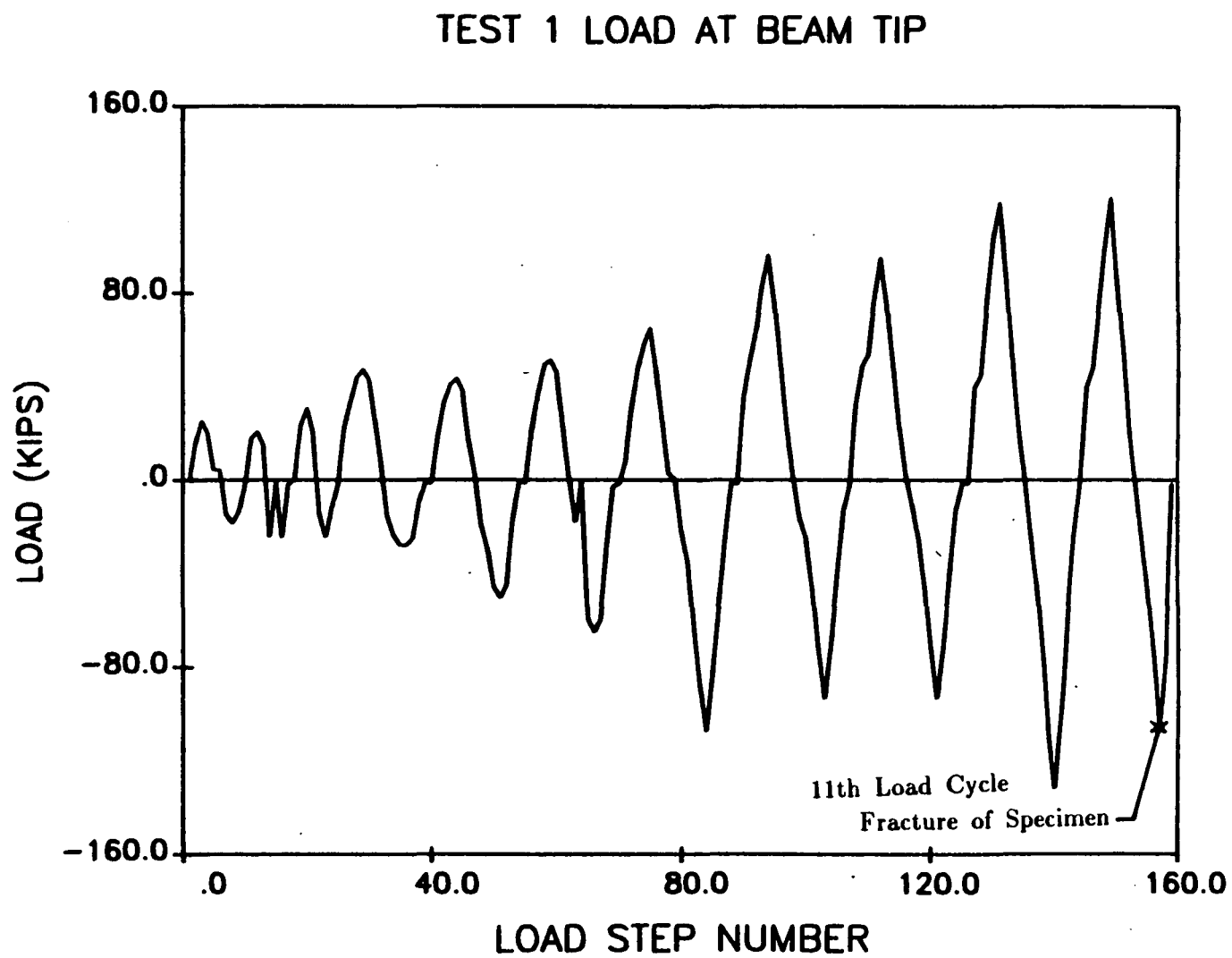


Figure A-5: Instrumentations for Tests

Figure A-6: Loading Sequence for Test 1





# TEST 2 LOAD AT BEAM TIP

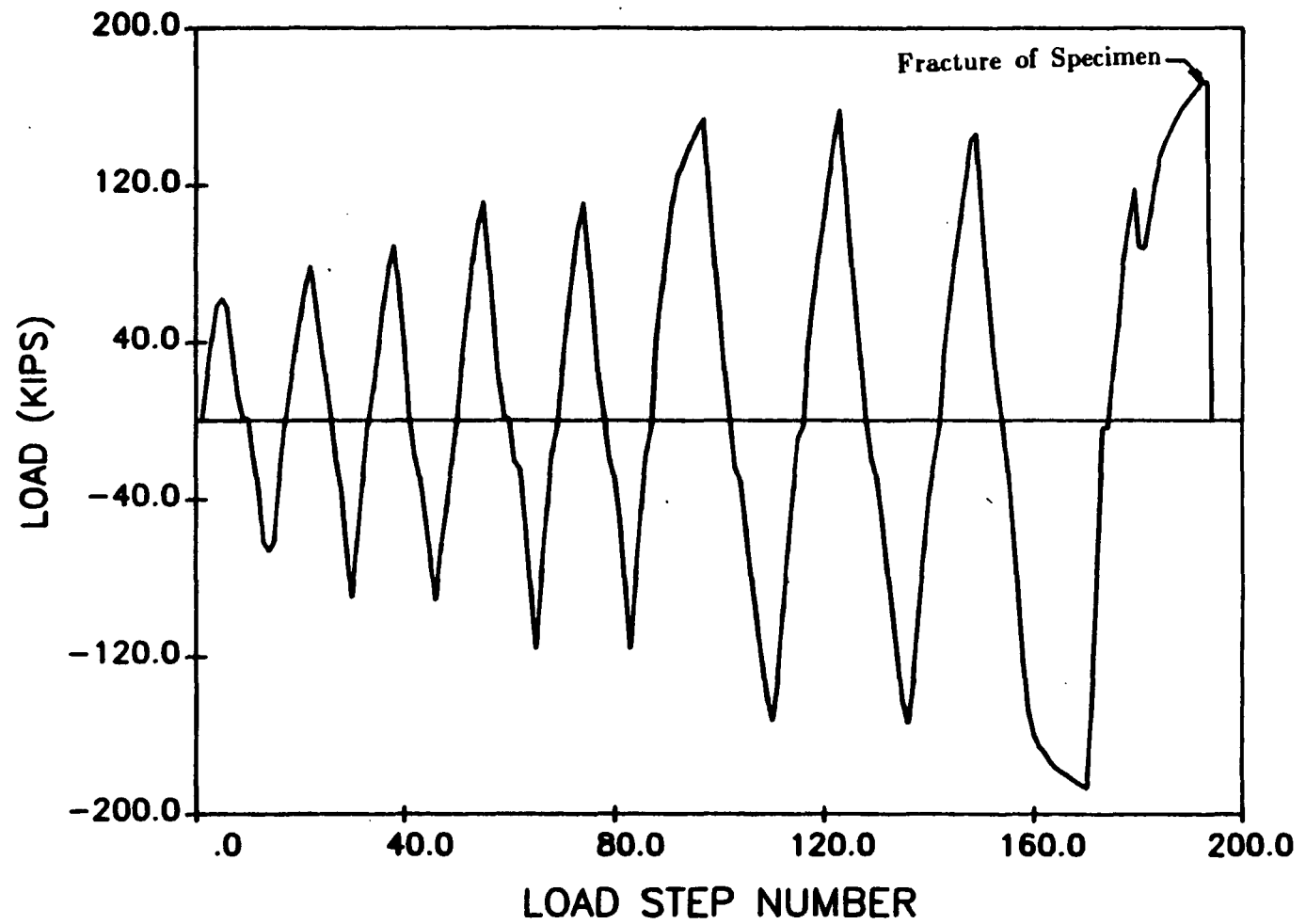


Figure A-7: Loading Sequence for Test 2

# TEST 3 LOAD AT BEAM TIP

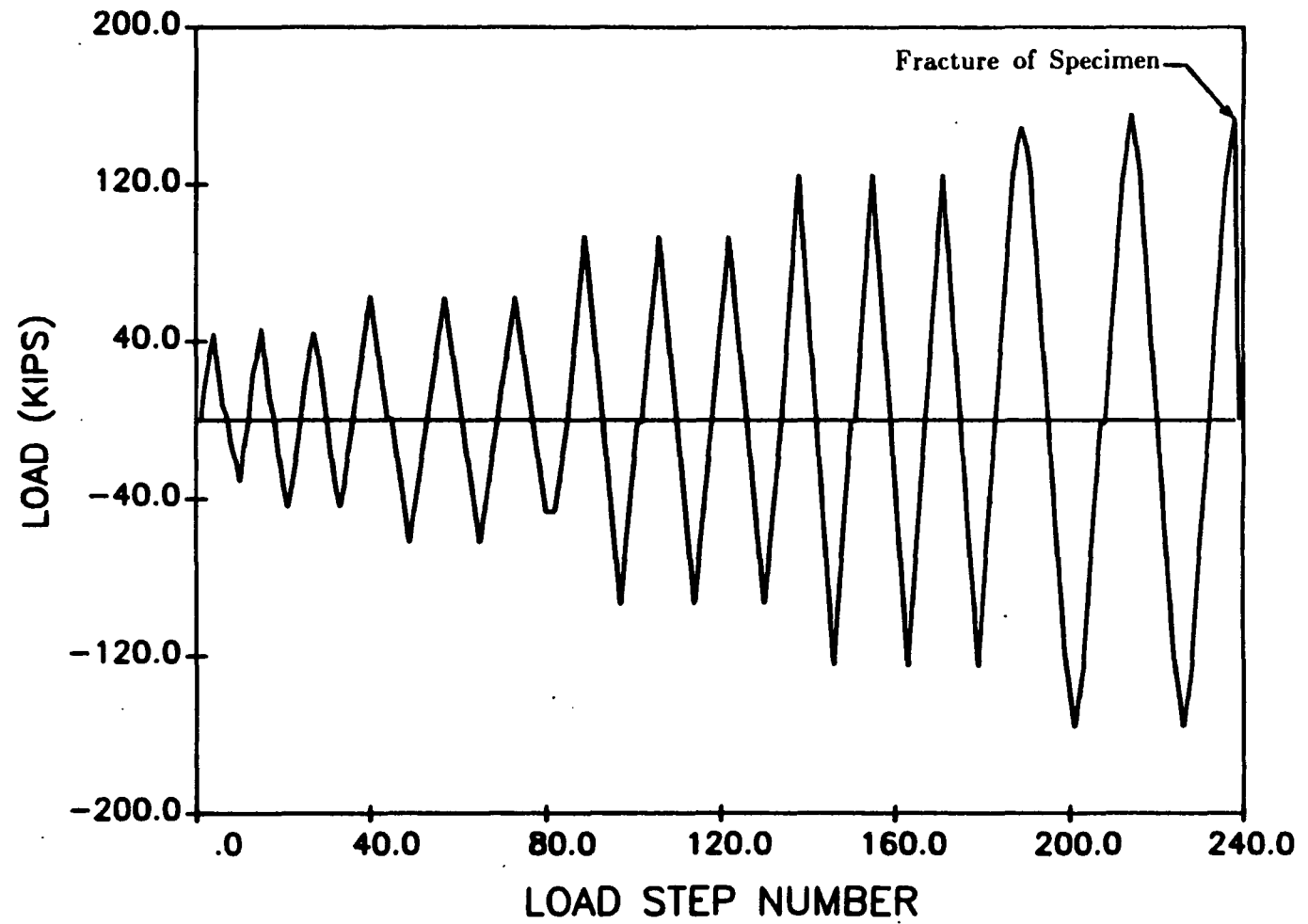


Figure A-8: Loading Sequence for Test 3

## T2 LOAD VERSUS DEFLECTION

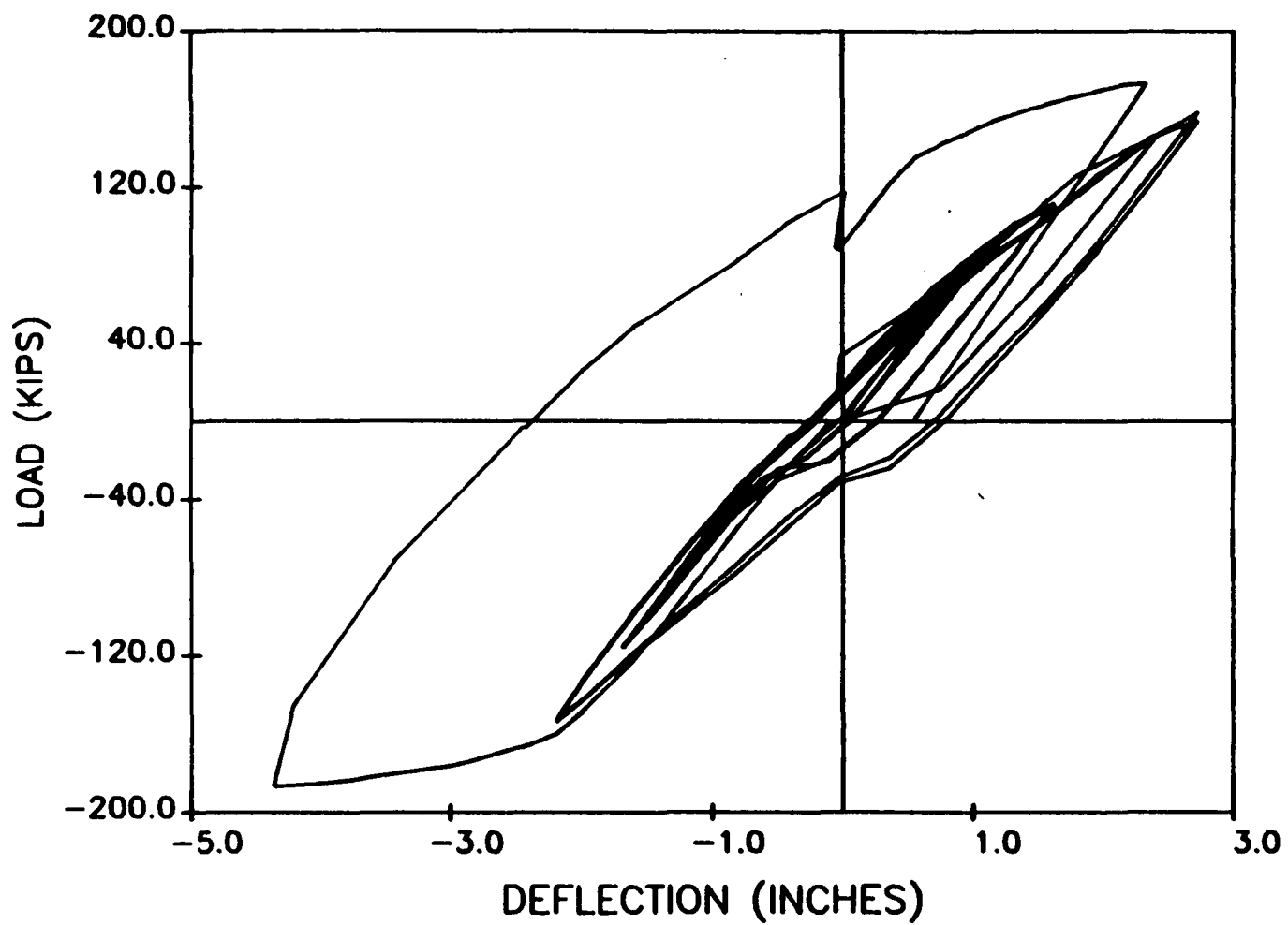


Figure A-9: Load-Deflection for Test 2

### T3 LOAD VERSUS DEFLECTION

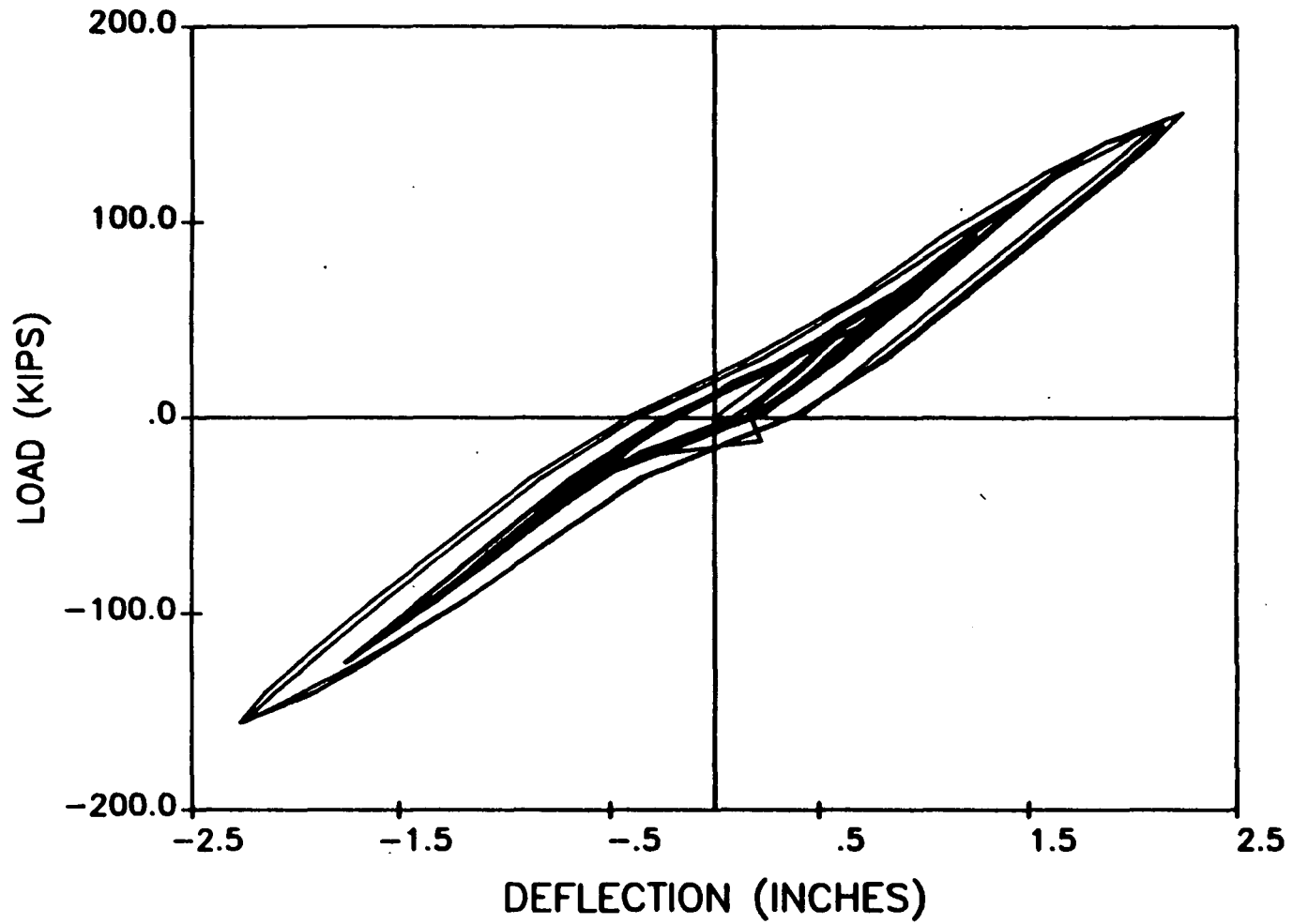


Figure A-10: Load-Deflection for Test 3

Figure A-11: STRUCTR Model for Connection Members

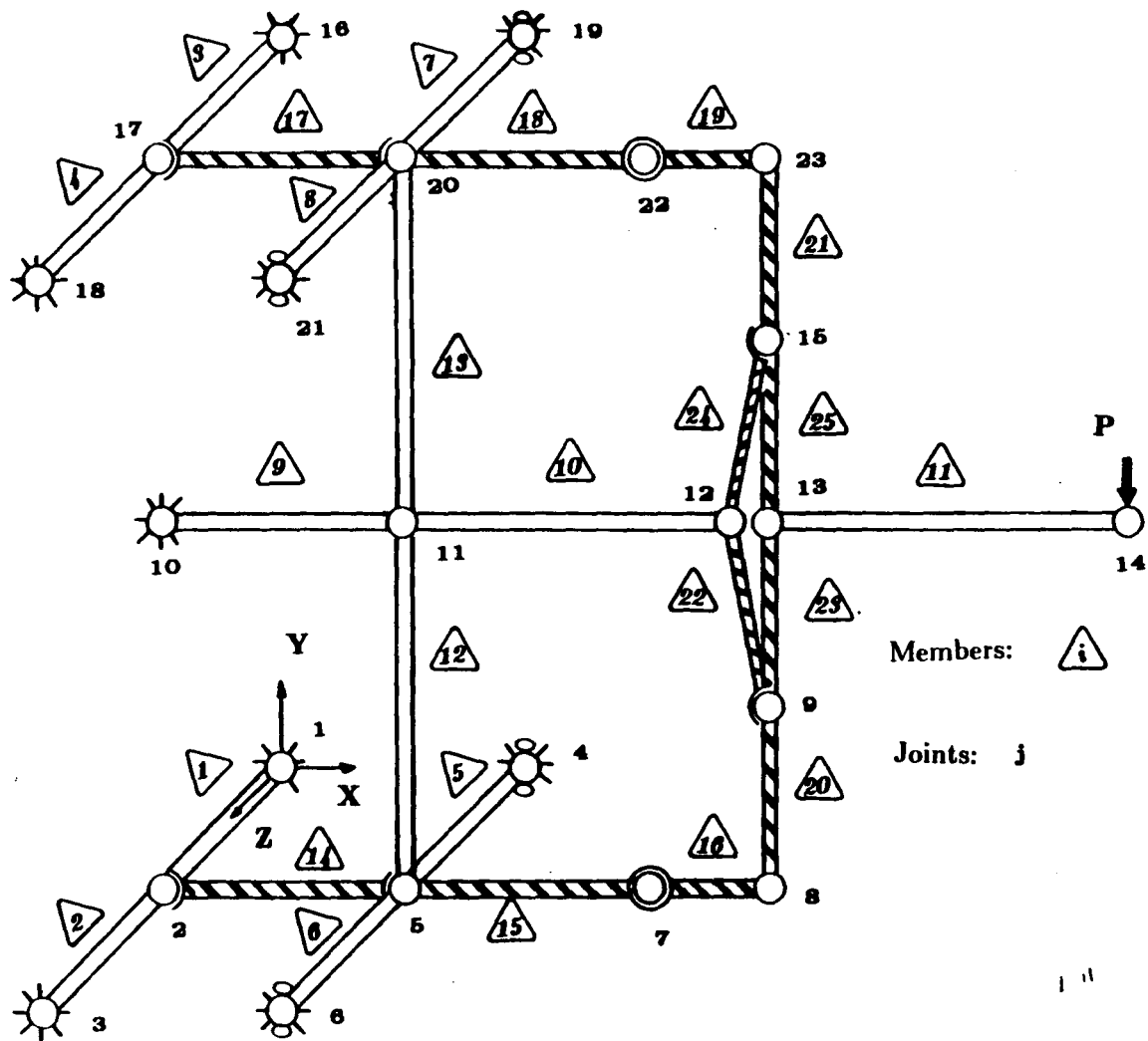


Figure A-12: Exploded Force Diagram for Connection Members

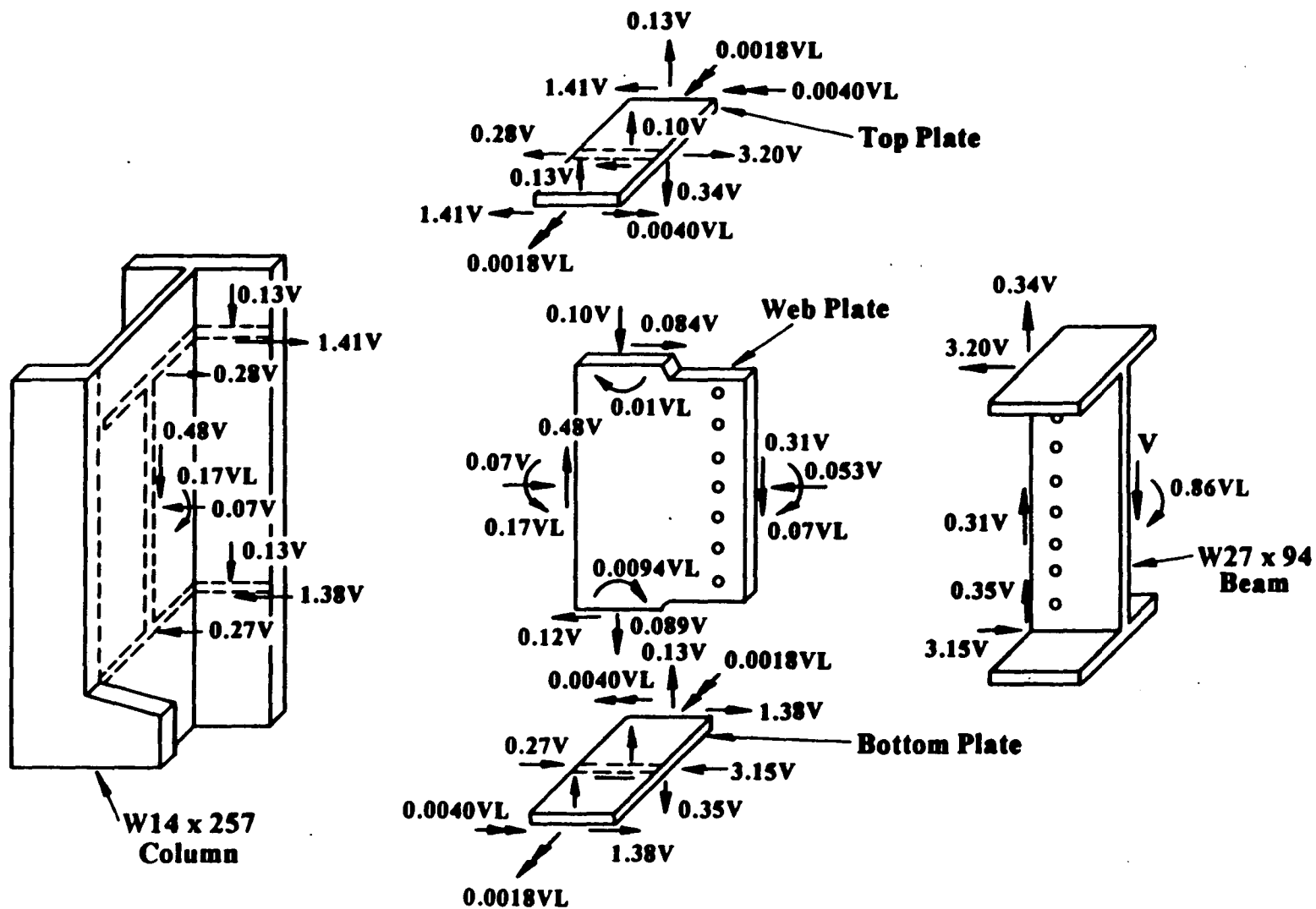
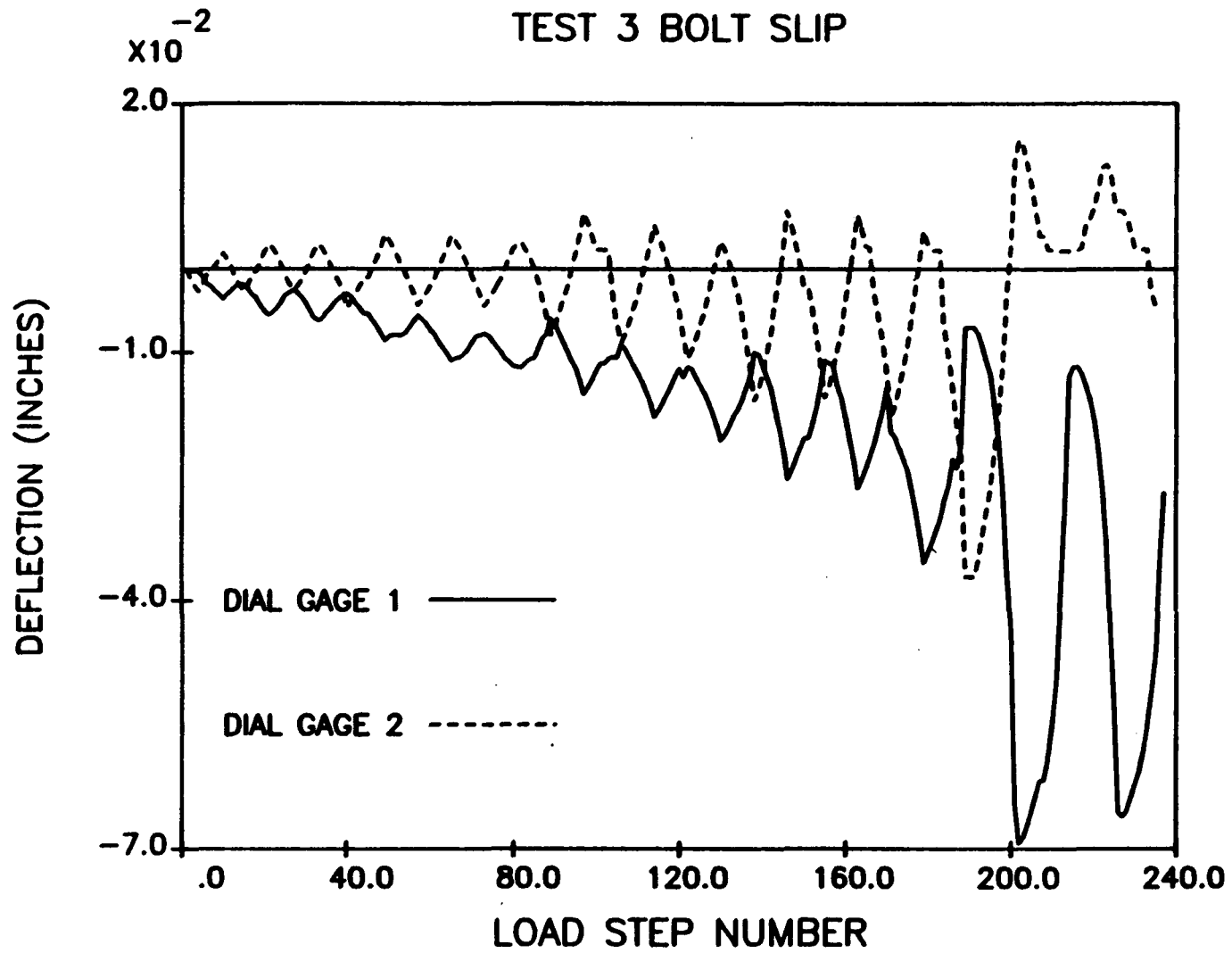


Figure A-13: Bolt Slip at Edges of Web Plate



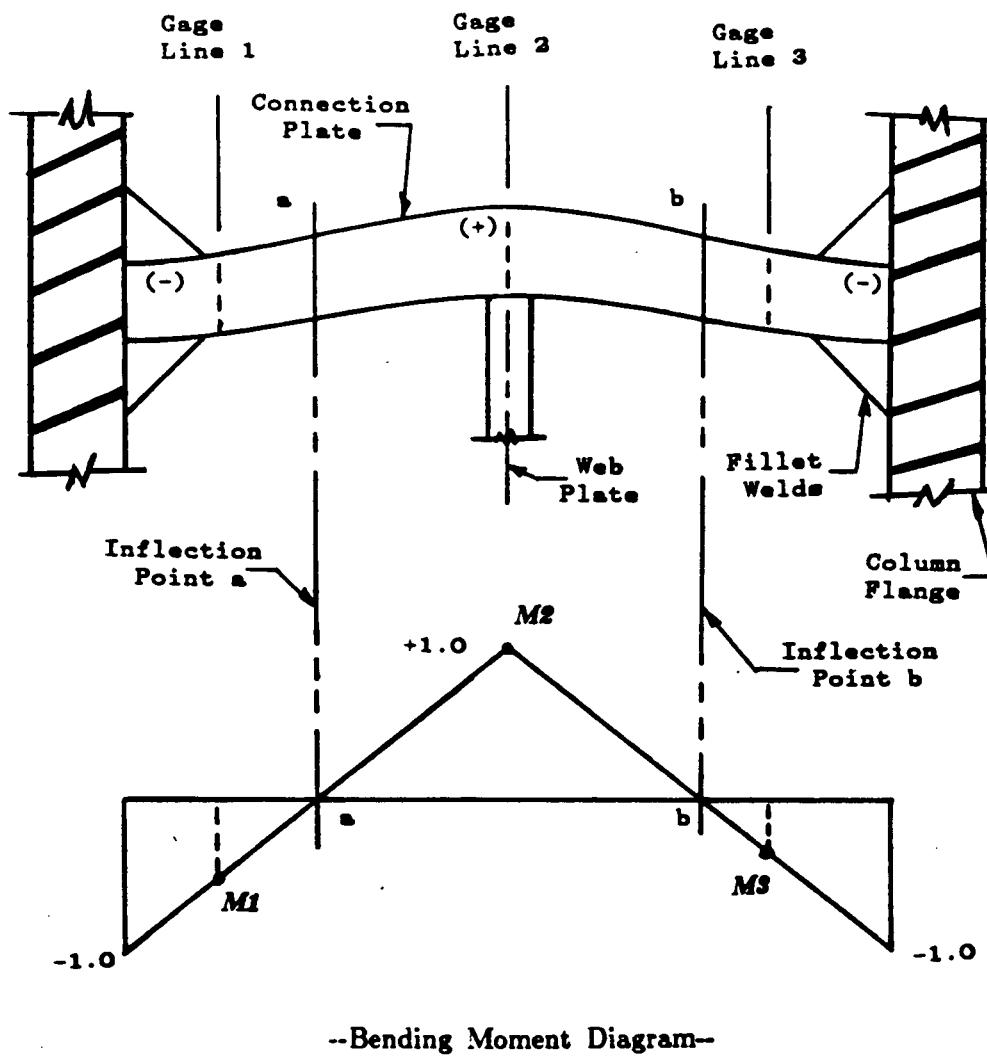


Figure A-14: Fixed End Beam Supports for Top Flange Plate



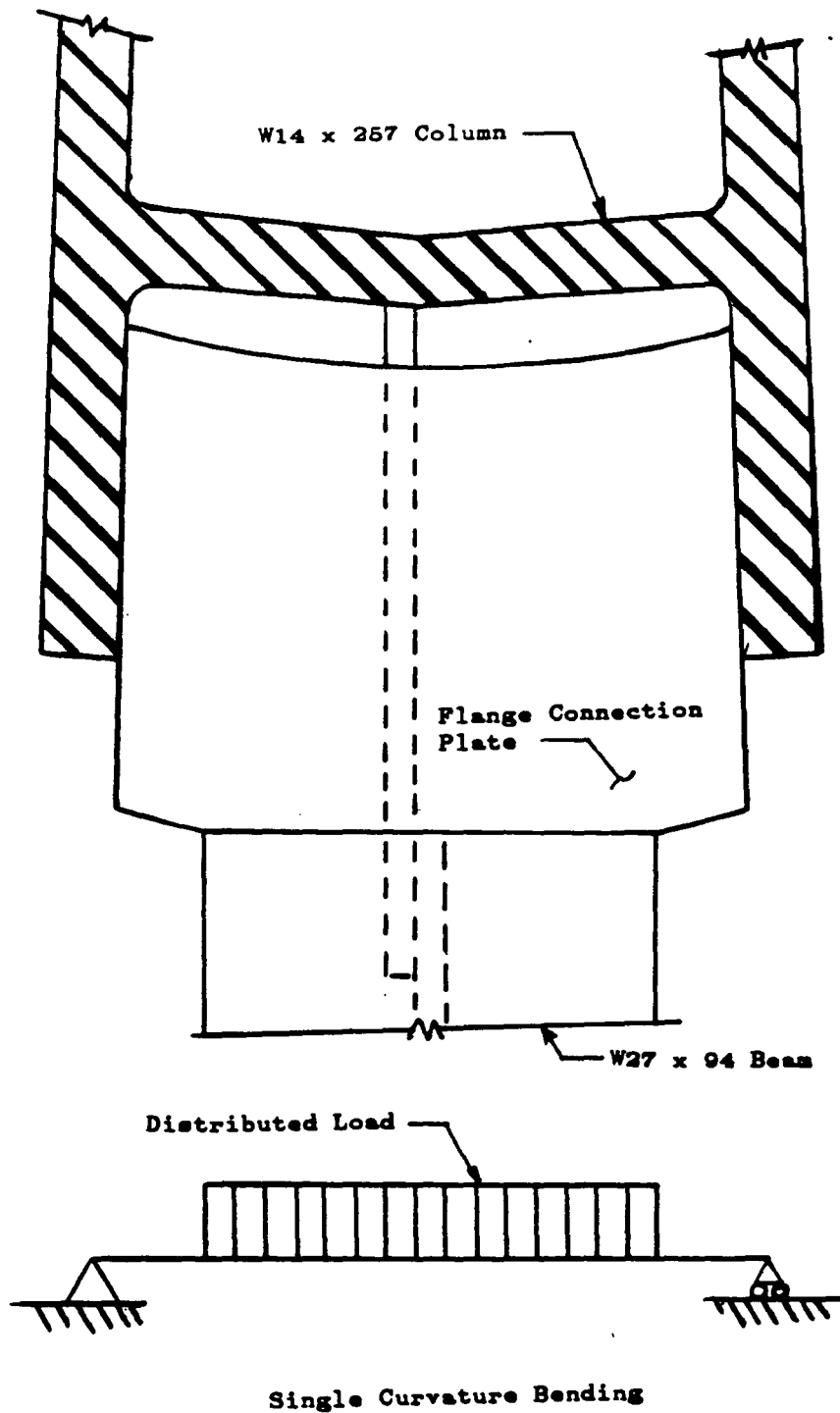


Figure A-15: Simple Span Bending of Top Flange Plate

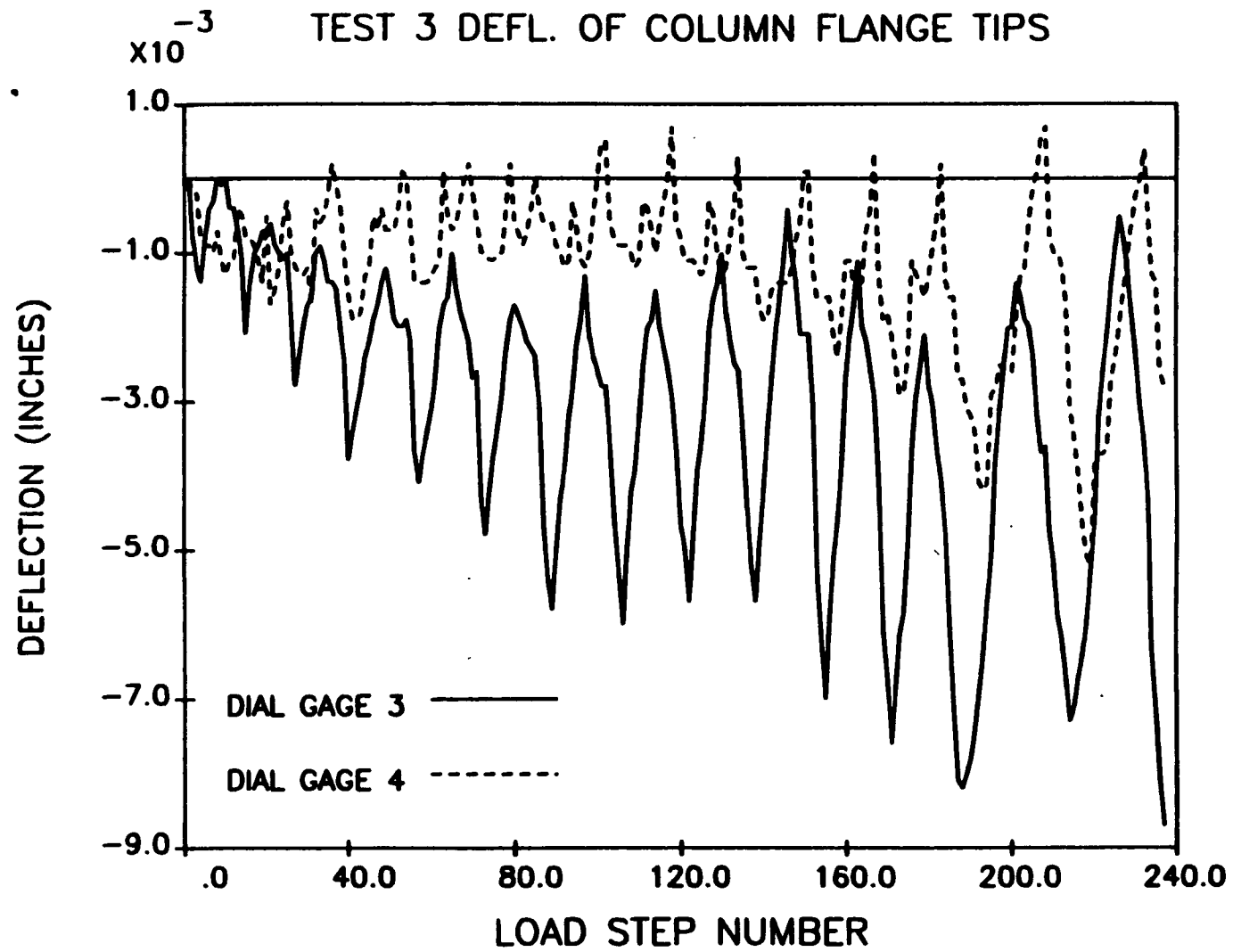


Figure A-16: Deflection at Column Flange Tips

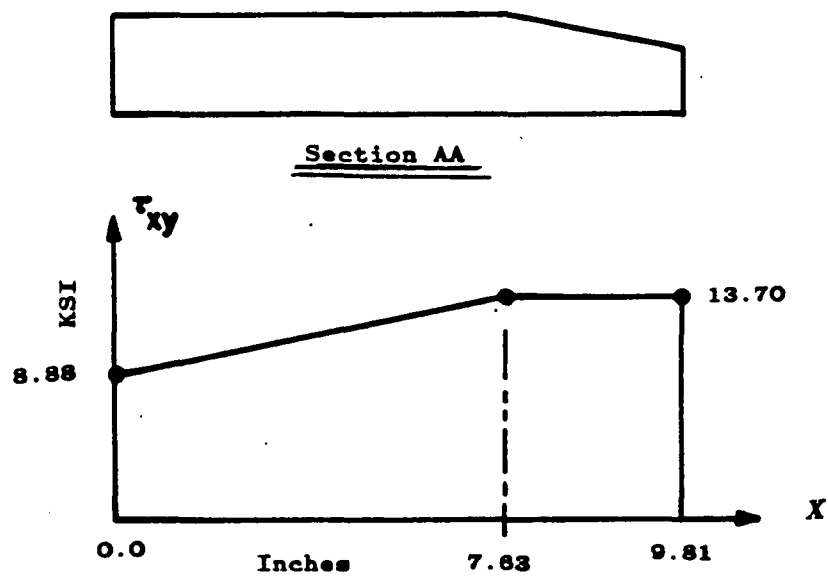
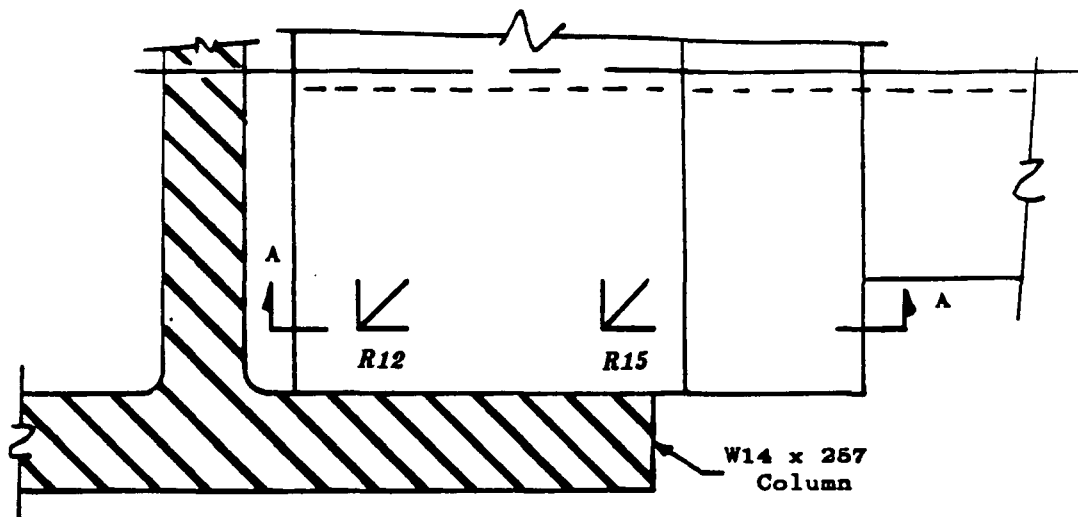


Figure A-17: Shear Stress Between Rosettes 12 & 15

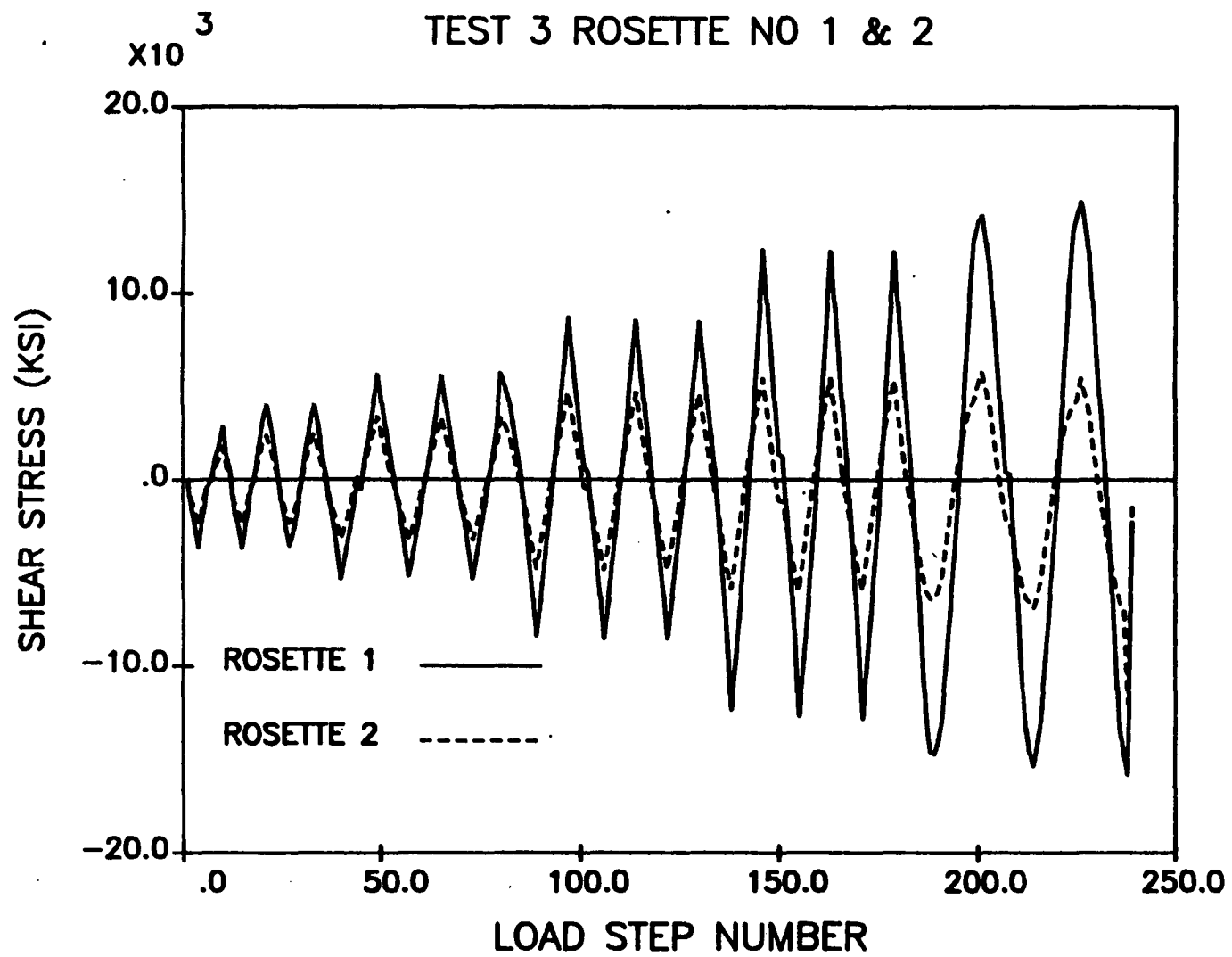


Figure A-18: Shear Stress Between Rosettes 1 & 2

Figure A-19: Shear Stress Between Rosettes 5 & 6

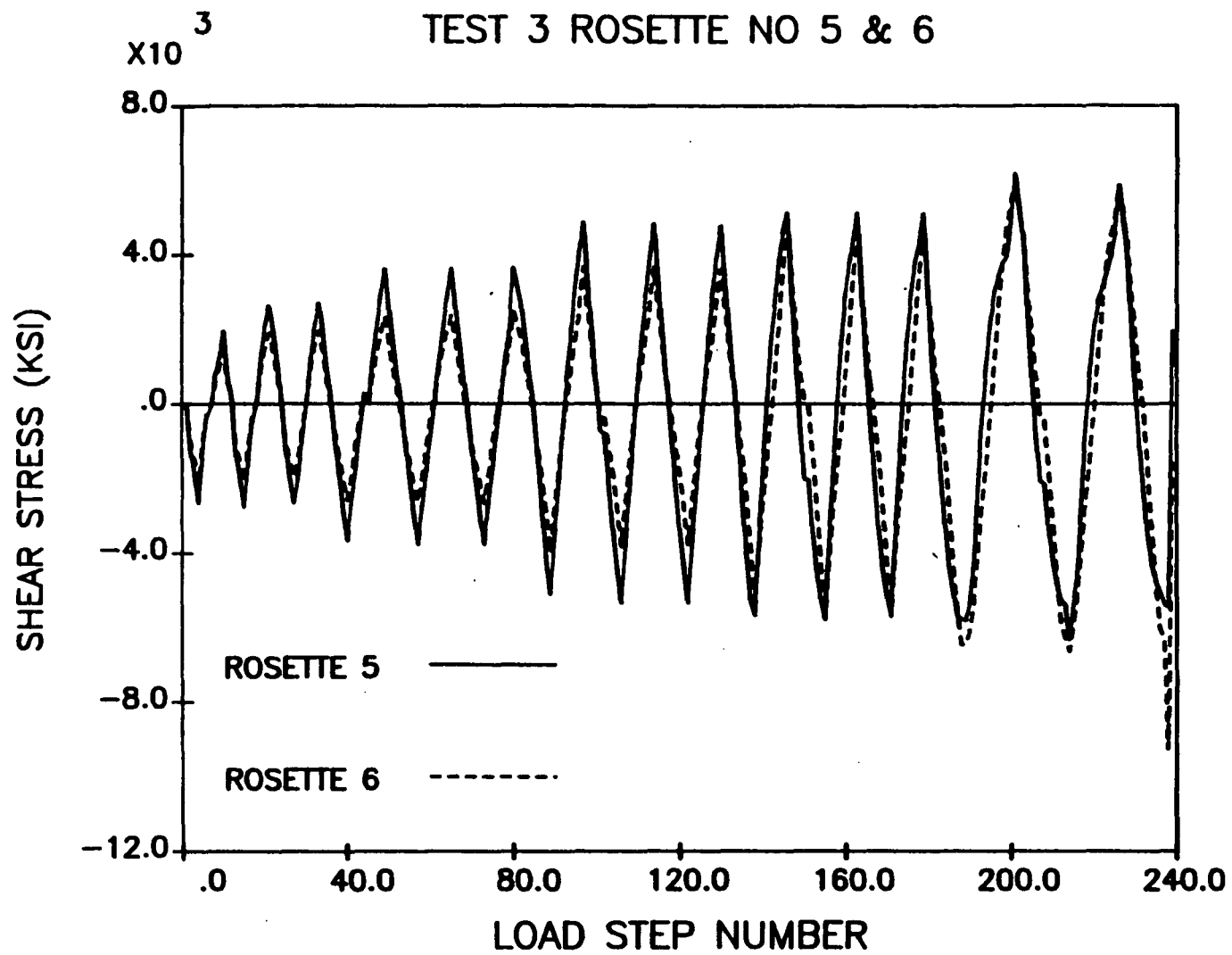
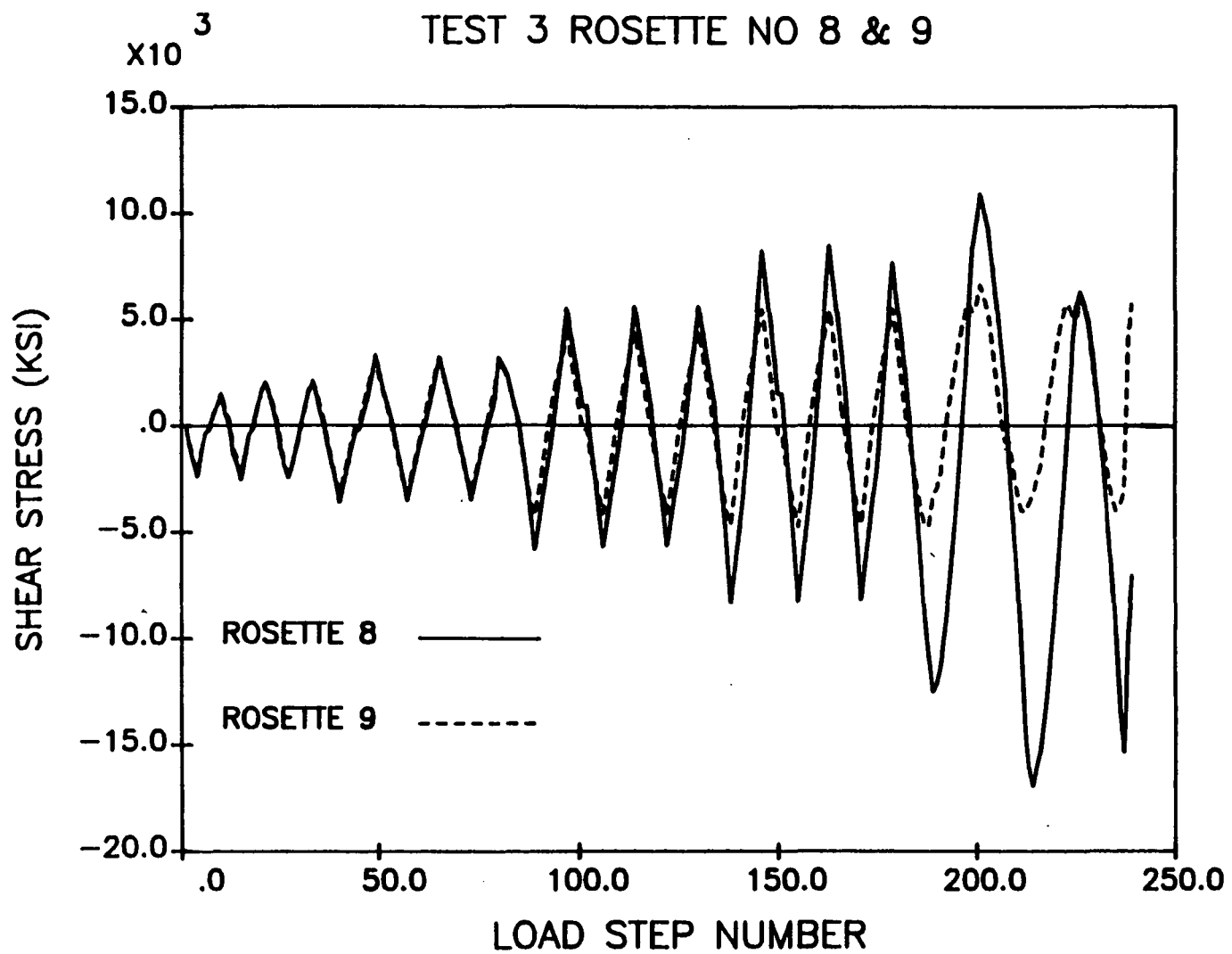


Figure A-20: Shear Stress Between Rosettes 8 & 9



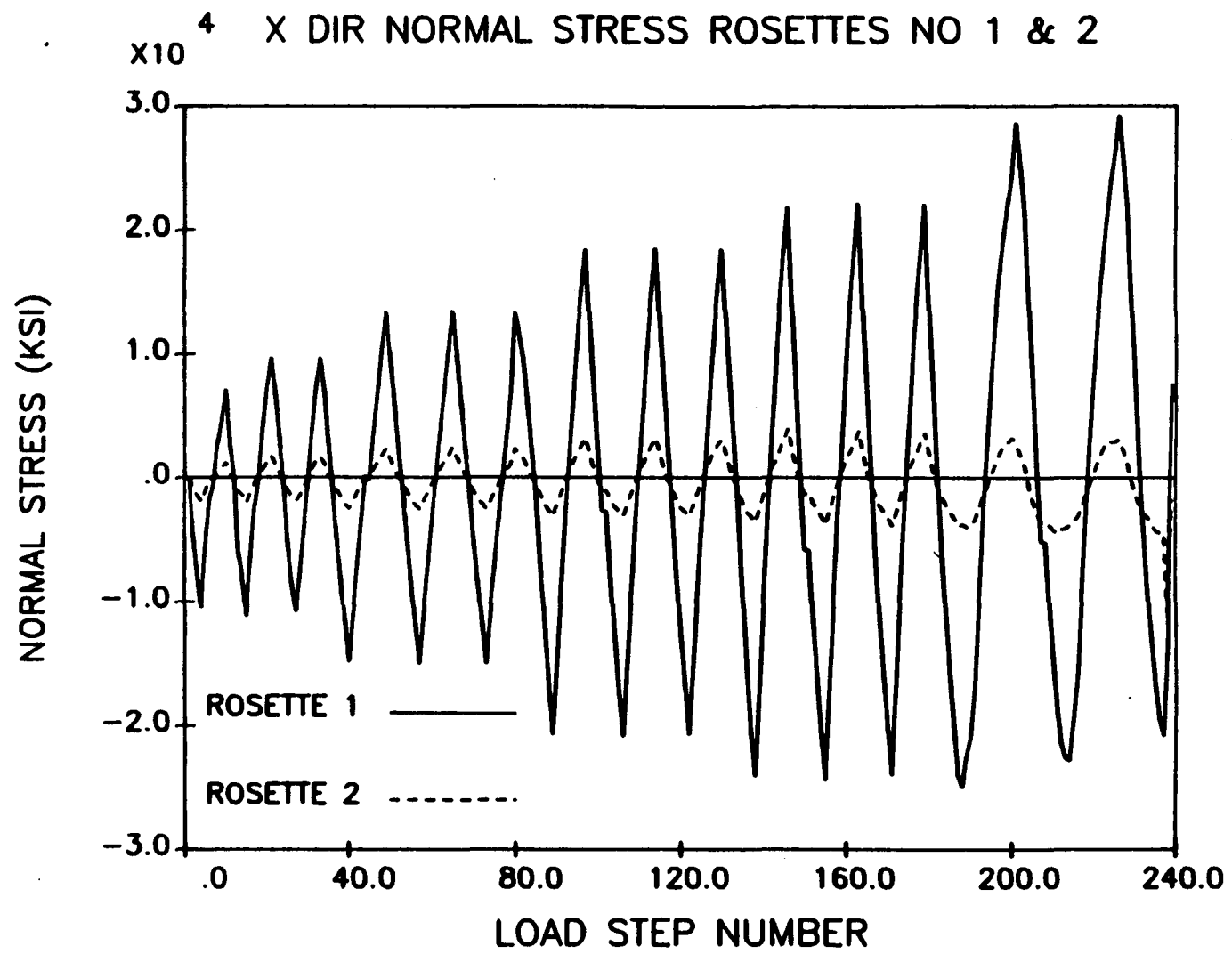


Figure A-21: Bending Stress Between Rosettes 1 & 2

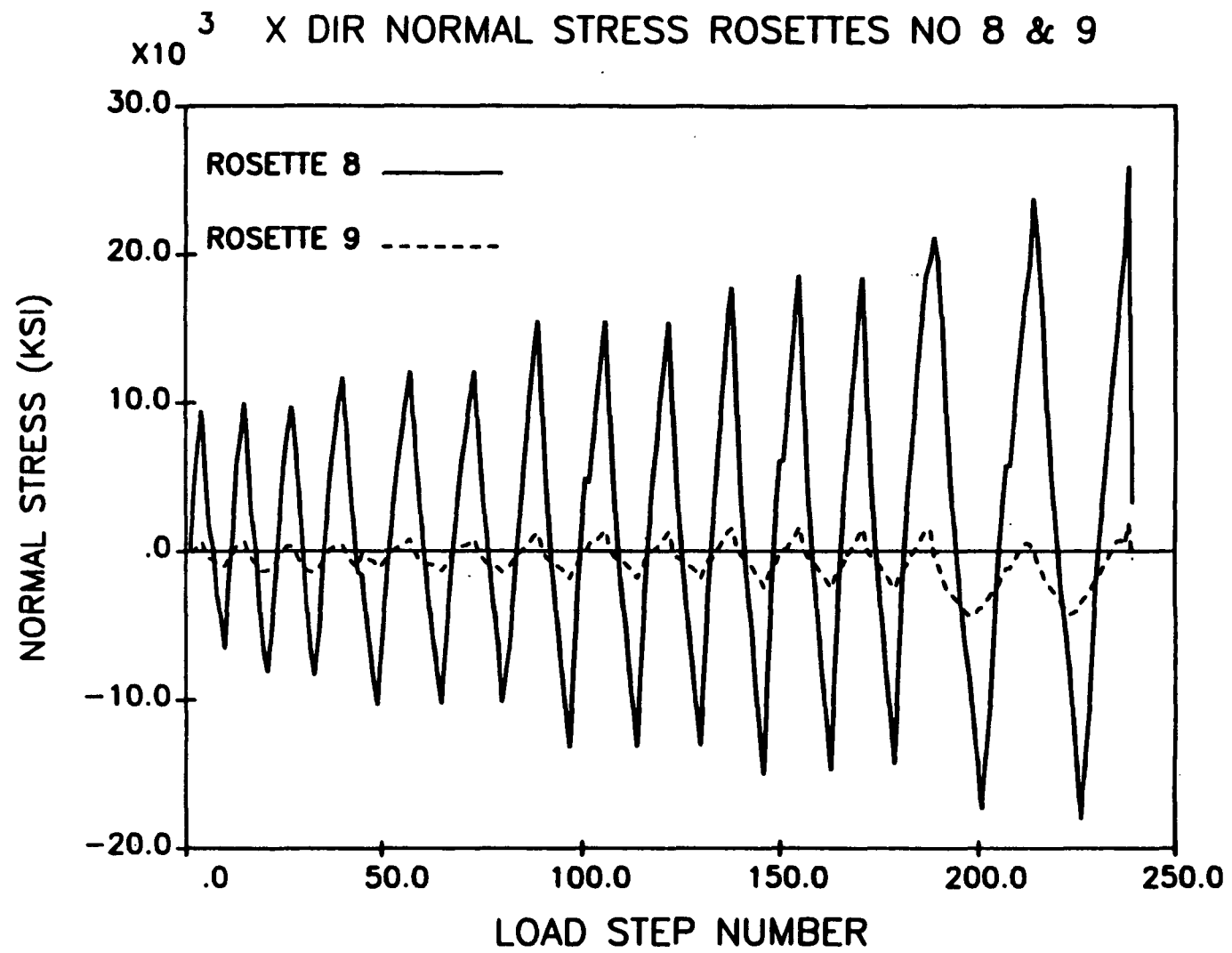


Figure A-22: Bending Stress Between Rosettes 8 & 9



Figure A-23: Stress Flow from Web to Flanges

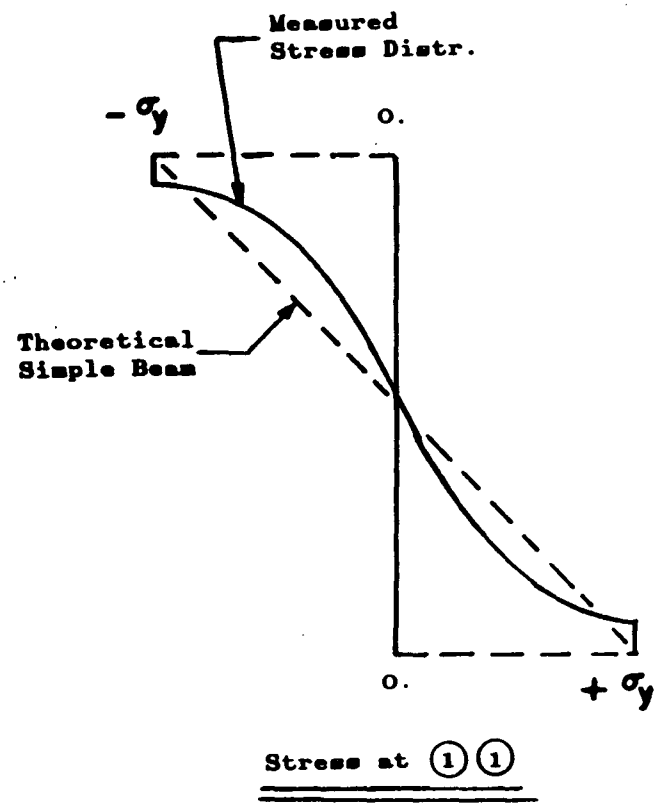
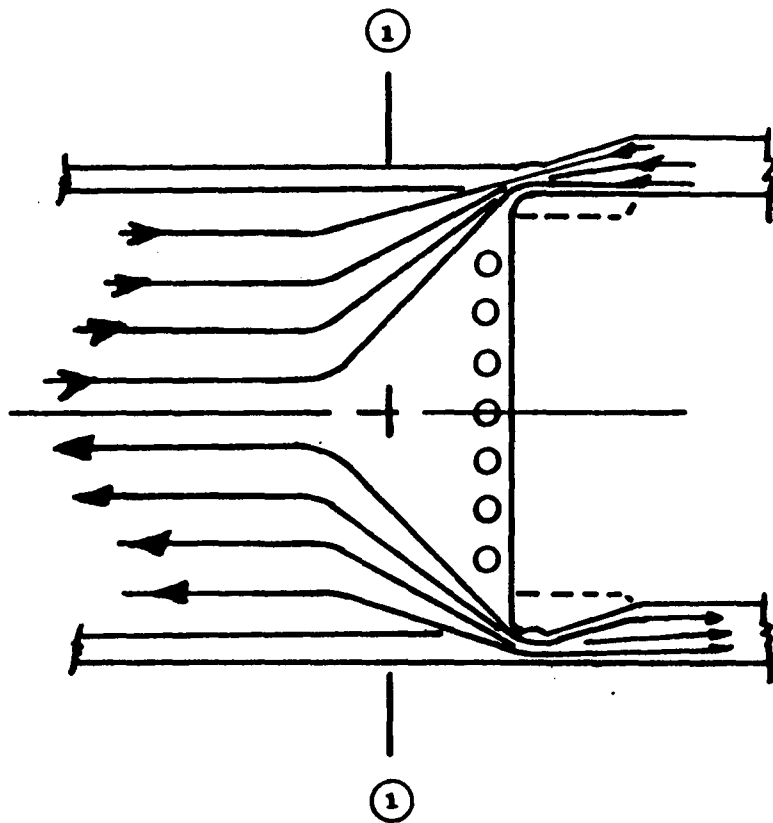
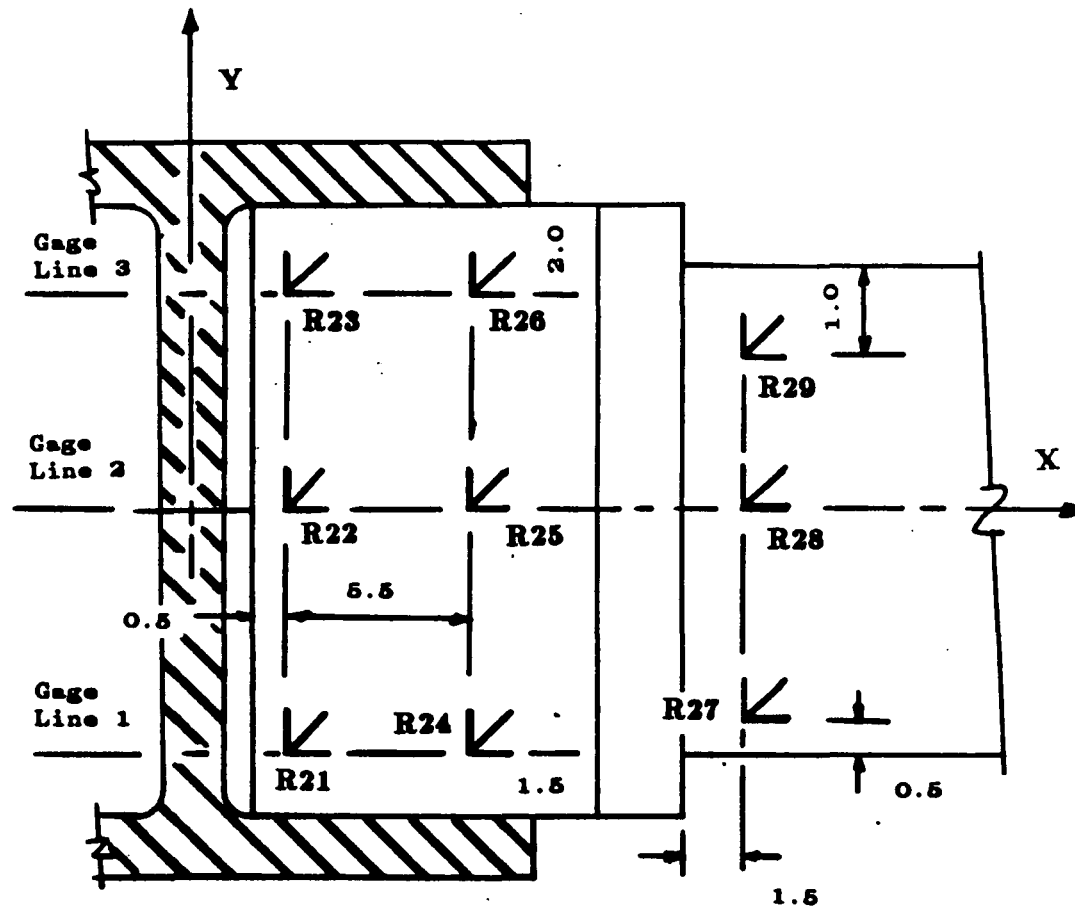


Figure A-24: Rosette Location of Bottom Flange



Note: All dimensions are in inches

Figure A-25: Bending Stress Between Rosettes 20 & 29

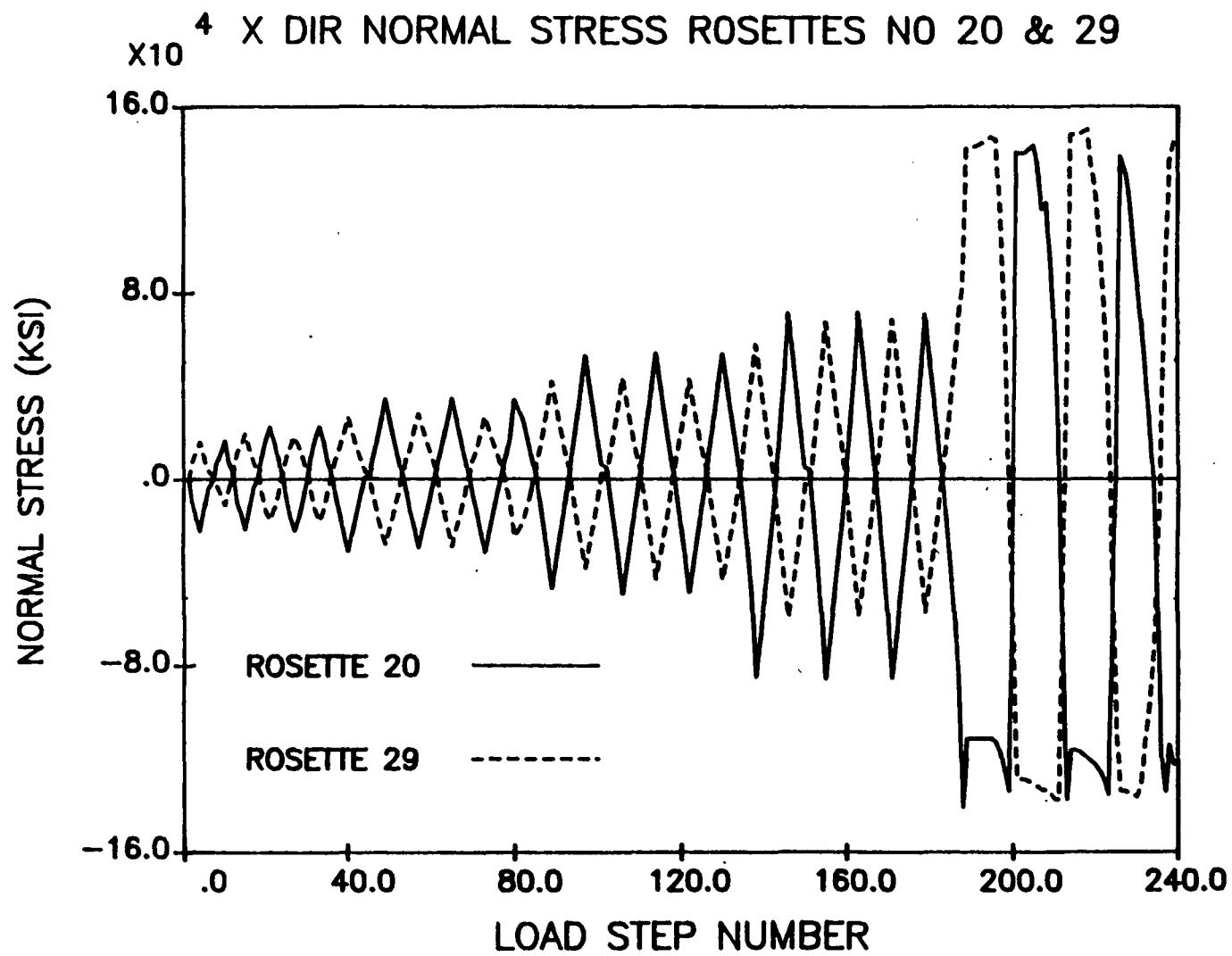
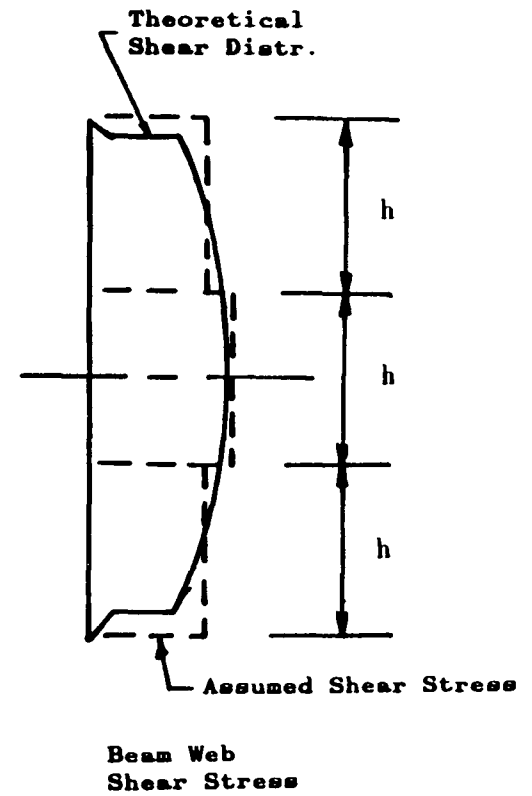
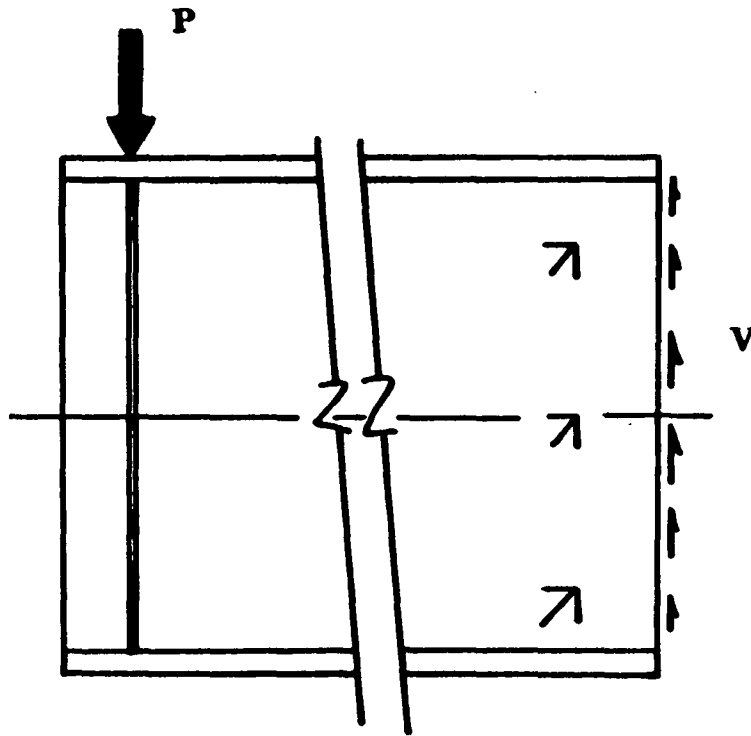


Figure A-26: Integration of Rosettes for Web Shear



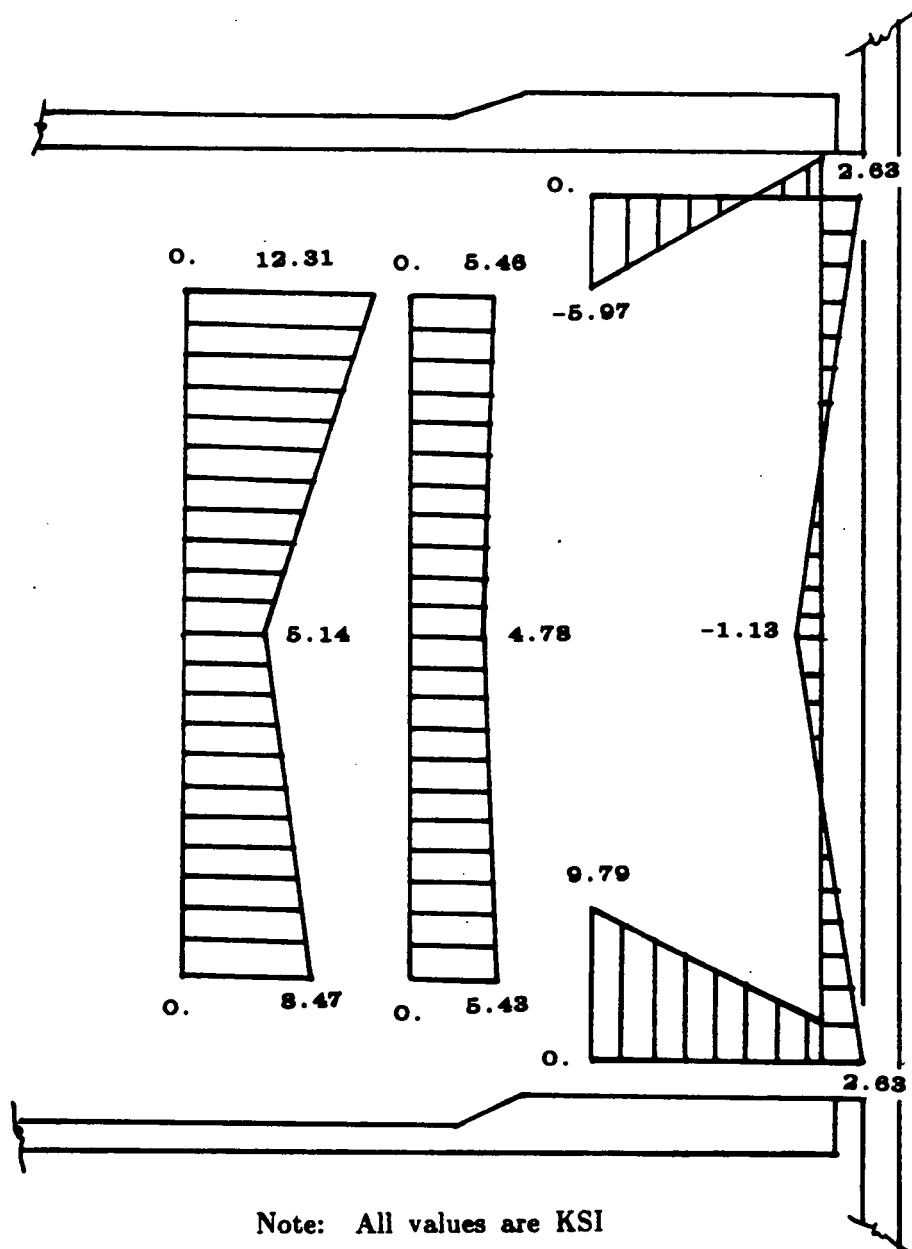


Figure A-27: Shear Stress Distribution in Beam Web

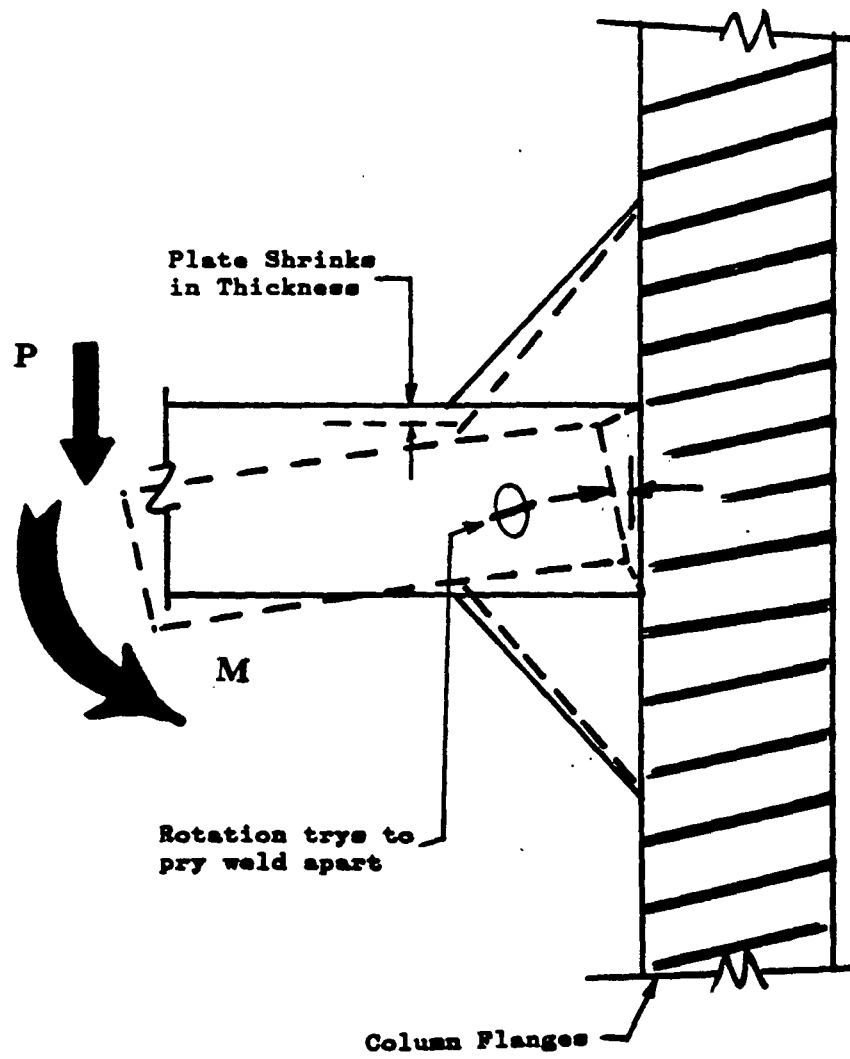
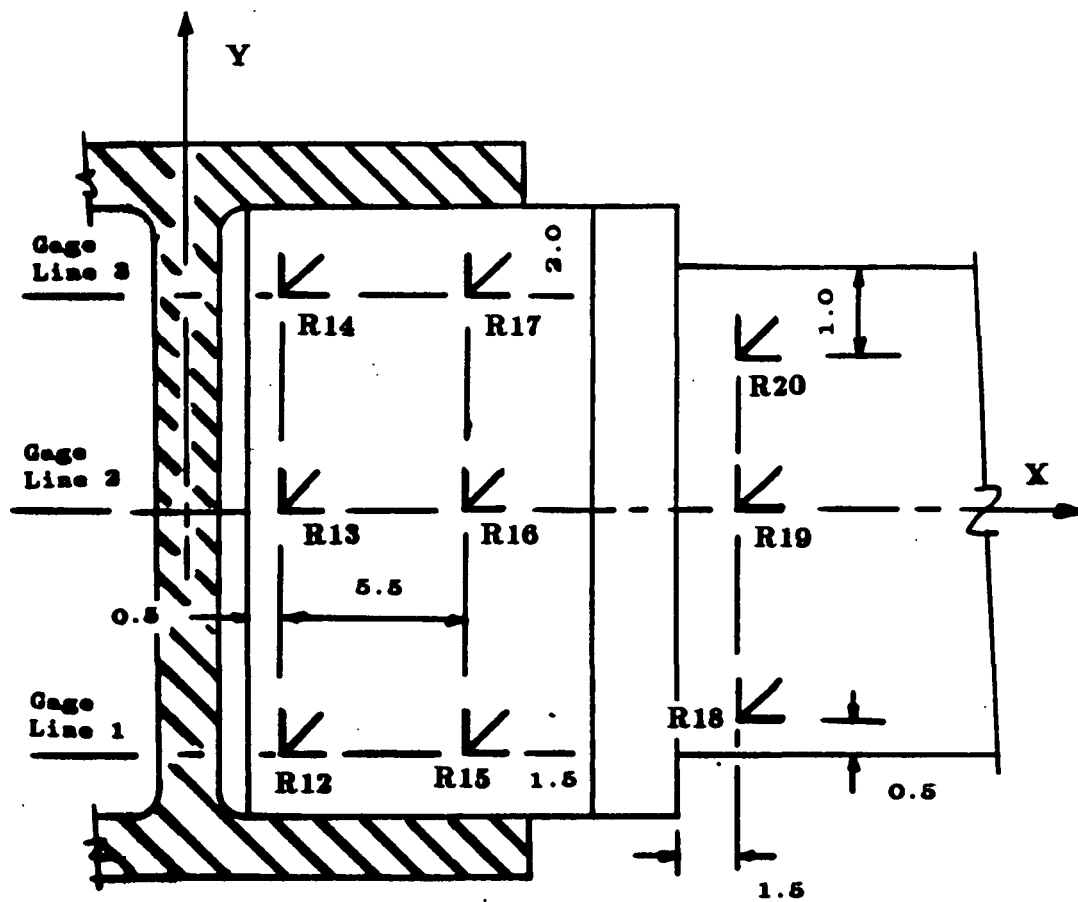


Figure A-28: Through-Thickness Restraint on Welds



Note: All dimensions are in inches

Figure A-29: Rosette Location on Top Flange

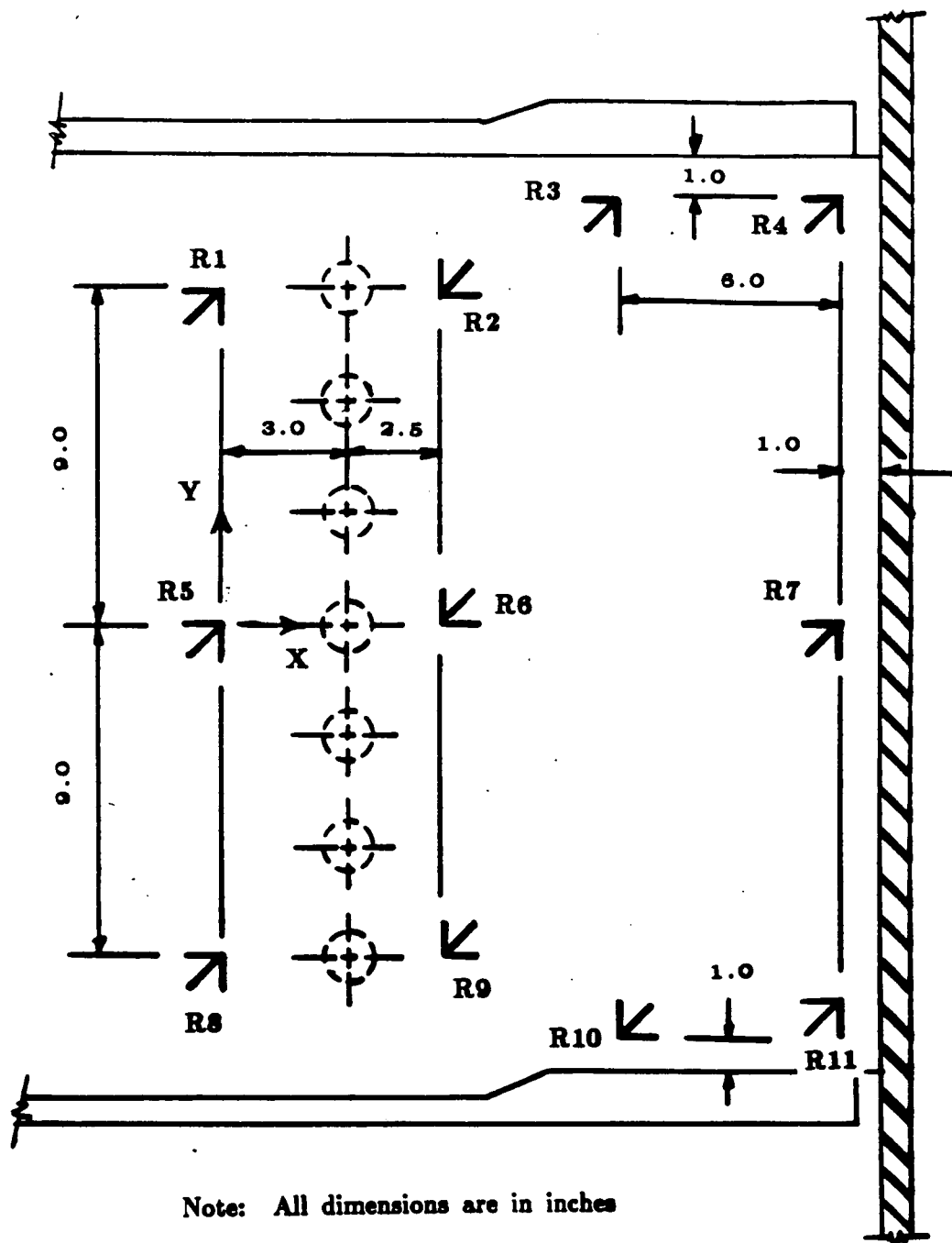
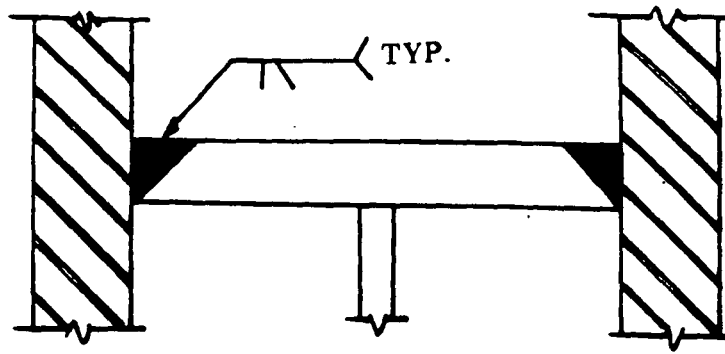
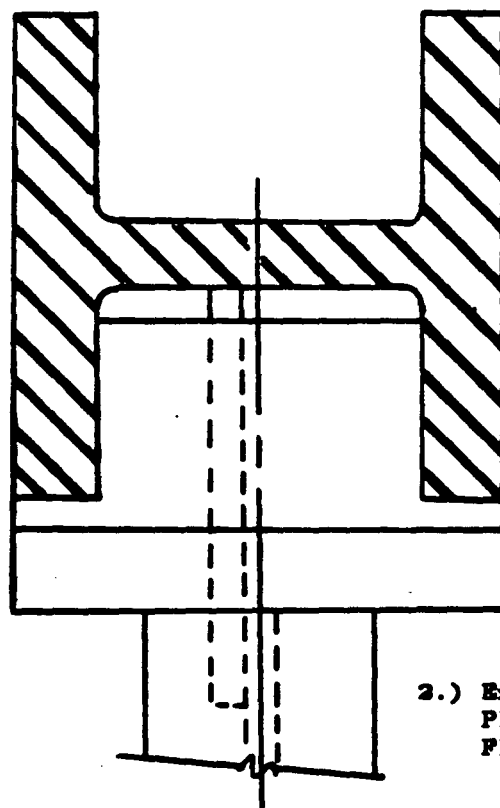


Figure A-30: Rosette Location on Beam Web





1.) Full Penetration Weld



2.) Extend Connection Plate Past Column Flange Tips

Figure A-31: Proposed Suggestions for Improvement

## Vita

The author was born in Sunbury, PA. on June 27, 1952 the first child of Blair L. and Marion W. Heaton. He graduated from Selinsgrove High School in 1970 and attended Lehigh University, Bethlehem, PA. where he received a Bachelor of Science degree in Civil Engineering in June, 1974.

The author was employed by Bechtel Power Corporation, Gaithersburg, MD., from June 1974 to October 1977, by Mid-Penn Engineering, Lewisburg, PA., from November 1977 to January 1979 and by Koppers Co., Williamsport, PA., from January 1979 to July 1985. He returned to Lehigh University in August 1985 to pursue a Master of Science Degree in Civil Engineering where he worked as a research assistant on Project. 504.